



















































CAPÍTULO 8

ANEXOS

ANEXO 1
ACRÓNIMOS

	BCR	Bureau Community of Reference
	Bkgrd	Muestra Representativa del Nivel de Fondo (Background sample)
	BQT	Bomba Química del Tiempo (Time Chemical Bomb)
	CCT	Tecnología de Celda de Colisión (Collision Cell Technology)
	CER	Factor de Enriquecimiento (Concentration Enrichment Ratio)
	CIC	Capacidad de Intercambio Catiónico (Cationic Exchange Capacity)
	CID	Dispositivo de Carga Inducida (Charge Injection Device)
	COD	Demanda Química de Oxígeno (Chemical Oxygen Demand)
	CRM	Material de Referencia Certificado (Certified Reference Material)
	CVAAS	Espectrometría de Absorción Atómica con Vapor Frío (Cold Vapor Atomic Absorption Spectrometry)
	DAB	Asfalto Cerrado (Dense Asphalt Bitumen)
	DCB	Ditionito, Citrato, Bicarbonato (Ditionite, Citrate Bicarbonate)
	ECG	Concentración/Valor Medioambiental Guía (Environmental Concentration Guideline)
	EDTA	Ácido Etilendiaminetetraacético (Ethylenediaminetetraacetic Acid)
	EPA	Agencia de Protección Ambiental (Environmental Protection Agency)
	ETAAS	Espectrometría de Absorción Atómica Electrotérmica (Electrothermal Atomic Absorption Spectrometry)
	ESR	Espectroscopia de Resonancia de Spin del Electrón (Electron Spin Resonance Spectroscopy)
	EXAFS	Espectroscopia de Absorción de Rayos X por Parte de la Estructura Fina (X-Ray Absorption Fine-Structure Spectroscopy)
	FAAS	Espectrometría de Absorción Atómica por Llama (Flame Atomic Absorption Spectrometry)
	HCA	Análisis de Clusters Jerárquico (Hierarchical Cluster Analysis)
	ICP-MS	Espectrometría de Masas por Plasma Acoplado Inductivamente (Inductively Coupled Plasma Mass Spectrometry).
	ICP-OES	Espectrofotometría de Emisión Óptica por Plasma Acoplado Inductivamente (Inductively Coupled Plasma Optical Emission Spectrophotometry).
	INAA	Análisis Instrumental de Activación Neutrónica (Instrumental Neutron Activation Analysis)

	ISO	Organización Internacional para la Estandarización (International Organization for Standardization)
	IUPAC	Unión Internacional para la Química Aplicada y Pura (International Union for Pure Applied Chemistry).
	KMO	Kaiser-Meyer-Olkin
	KS	Kolmogorov-Smirnov
	LOD	Límite de Detección (Limit of Detection)
	LOQ	Límite de Cuantificación (Limit of Quantification)
	MCE	Mezcla Celulosa Ester (Mixed Cellulose Ester)
	MOB	Movilidad a Largo Plazo (Long Term Mobility)
	MOPU	Ministerio de Obra Públicas
	NBS	Comité Nacional de Estándares (National Bureau of Standards)
	NIPALS	No Linear Iterativo de Mínimos Cuadrados (Non-Linear Iterative Partial Least Squares)
	NIST	Instituto Nacional de Estándares y Tecnología (National Institute of Standards & Technology)
	OMS	Organización Mundial para la Salud (World Health Organization)
	PAHs	Hidrocarburos Policíclicos Aromáticos (Polycyclic Aromatic Hydrocarbons)
	PC	Componente Principal (Principal Component)
	PCA	Análisis de Componentes Principales (Principal Components Analysis)
	PET	PentaEritriol (PenthaEriTriol)
	PFA	Perfluoroalcoxy
	RDS	Sedimento Depositado junto a Carretera (Roadside Deposited Sediment)
	RSD	Desviación Estándar Relativa (Relative Standard Deviation)
	RMN	Resonancia Magnética Nuclear (Nuclear Magnetic Resonance)
	SCD	Dispositivo de Carga Acoplada (Segmented-Array Charged-Coupled Device)
	SEM/EDX	Microscopía Electrónica con Espectrometría de Dispersión de Rayos-X (Scanning Electron Microscopy with Energy Dispersive X-Ray Spectrometry)
	SES	Esquema de Extracción Secuencial (Sequential Extraction Scheme).
	SM&T	Programa de Medidas y Test de Estándares (Standard Measurements and Testing Programme)
	SRM	Material de Referencia Estándar (Standard Reference Material)
	TDS	Sólidos Totales Disueltos (Total Dissolved Solids)

	TPA	Tecnología de Protección Ambiental
	XRF	Fluorescencia de Rayos X (X-Ray Fluorescence)
	XPS	Espectroscopia fotoelectrónica de Rayos X (X-Ray Photoelectron Spectroscopy)
	ZOAB	Asfalto Abierto Poroso (Zeer Open Asphalt Bitumen)

ANEXO 2

ÍNDICE DE FIGURAS Y TABLAS

Capítulo 1. Introducción.

FIGURAS

Figura 1.1 Ejemplo de un ciclo biogeoquímico	17
Figura 1.2 Evolución en la producción industrial de metales pesados a lo largo del siglo XX (Ton ·año ⁻¹).....	20
Figura 1.3 Distribución estadística de los metales presentes en zonas contaminadas.....	21
Figura 1.4 Causas y efectos de la contaminación en suelos.....	22
Figura 1.5 Diagrama del ciclo de contaminación medioambiental y remediación. 1) Percepción científica. 2) Percepción sociopolítica. 3) Acción gubernamental. 4)Inicio de la disminución de la contaminación. 5) Logro de niveles básicos estipulados.....	37
Figura 1.6 Relación entre la movilidad de los metales en las distintas fases y la fuerza extractante de los reactivos comúnmente empleados en los SES.....	54
Figura 1.7 Patrón de fraccionamiento de un material de referencia certificado, CRM BCR 601, tras la aplicación de un SES. F1) Fracción intercambiable; F2) Fracción reducible; F3) Fracción oxidable; F4) Fracción residual.....	57
Figura 1.8 Matrices comúnmente estudiadas al aplicar SES. Datos primarios extraídos de Filgueiras, A., et al.....	57
Figura 1.9 Patrones espaciales en W y X para la toma de muestra sistemática.....	69
Figura 1.10 Plantillas especiales para la toma de muestra sistemática.....	70

TABLAS

Tabla 1.1 Concentraciones medias de As, Cd, Cr, Cu, Ni, Pb y Zn observadas en matrices medioambientales de origen geológico (µg ·kg ⁻¹).....	19
Tabla 1.2 Actividades industriales y comerciales que potencialmente pueden generar problemas de suelos contaminados.....	19
Tabla 1.3 Fuentes de contaminación antropogénica de suelos y sedimentos.....	20
Tabla 1.4 Índices tecnofílicos para metales con aportación favorecida antropogénicamente.....	20
Tabla 1.5 Listado de las causas y efectos de la contaminación en suelos expuestos en la Figura 1.4.....	22
Tabla 1.6 Metales esenciales y tóxicos para los mamíferos. * En forma de As(III), As(V), etc.....	24
Tabla 1.7 Toxicidad relativa de los metales en mamíferos.....	24
Tabla 1.8 Principales síntomas de deficiencia y toxicidad provocados por algunos elementos.....	25
Tabla 1.9 Grado de movilidad de diferentes elementos traza bajo diferentes condiciones medioambientales.....	34
Tabla 1.10 Concentraciones máximas permitidas legislativamente de metales para fangos de estaciones depuradoras apropiados para disponer con fines agrícolas y metales en suelos tratados con fangos de estaciones depuradoras, en diferentes países de la comunidad económica europea. (mg ·kg ⁻¹).....	39
Tabla 1.11 Niveles máximos permitidos (mg ·kg ⁻¹) legalmente de metales pesados en suelos por diferentes instituciones europeas en función del uso del suelo.....	40
Tabla 1.12 Principales características de los análisis de especiación en función del área de aplicación. Dicha tabla se proporciona como muestra de las diferentes acepciones del término especiación.....	43
Tabla 1.13 Reactivos comúnmente utilizados para la extracción de metales asociados a la fracción intercambiable.....	46
Tabla 1.14 Reactivos comúnmente utilizados para la extracción de metales asociados a la fracción de los carbonatos.....	47
Tabla 1.15 Reactivos comúnmente utilizados para la extracción de metales asociados a óxidos de hierro y manganeso.....	49
Tabla 1.16 Reactivos comúnmente utilizados para la extracción de metales asociados a la materia orgánica.....	51
Tabla 1.17 Reactivos comúnmente utilizados para la digestión y extracción de metales asociados a la fracción residual.....	53
Tabla 1.18 Reactivos más comúnmente empleados en las distintas fracciones de los procedimientos de extracción secuencial. Adaptado de Kersten and Förstner.....	55
Tabla 1.19 Descripción de las condiciones experimentales de los procedimientos de extracción secuencial originales de Tessier y del Bureau Community of Reference.....	59
Tabla 1.20 Preguntas relevantes para diseñar un plan de muestreo.....	67
Tabla 1.21 Posibles fuentes de error en la planificación y realización de la toma de muestra.....	68
Tabla 1.22 Parámetros edafológicos determinantes de la capacidad del suelo para acumular metales pesados y compuestos orgánicos tóxicos.....	71
Tabla 1.23 Parámetros complementarios de la caracterización del suelo.....	71

Capítulo 2. Experimental.

FIGURAS

Figura 2.1 Representación de los ICP-OES empleados en este estudio. A) ARL 3410; B) Perkin Elmer 4300 DV Optima; C) ThermoElemental Intrepid II XSP.....	100
Figura 2.2 Corte esquemático del diseño estructural del equipo ICP-MS ThermoElemental PQ-ExCell utilizado en los estudios que se presentan.....	102
Figura 2.3. Esquema de los componentes de un vaso de reacción de PFA para microondas analítico.....	108
Figura 2.4. Descripción del funcionamiento del PCA, mostrando los loadings (p_i) y los scores (t_i).....	112
Figura 2.5. Diagrama doble de loadings (p_i) y scores (t_i) para el conjunto de PC1 y PC2.....	114
Figura 2.6. Representación gráfica de un dendograma.....	115
Figura 2.7. Sumario de condiciones experimentales correspondientes a los Esquemas de Extracción Secuencial del BCR (A) y del SM&T (B).....	119
Figura 2.8. Sumario de condiciones experimentales correspondientes a los Esquemas de Extracción Secuencial Monoetapa del BCR (A) y del SM&T (B).....	120

TABLAS

Tabla 2.1. Características de las técnicas analíticas empleadas según bibliografía. ¹¹ Los valores del límite de detección son evaluados según el criterio 3σ para muestras ideales. Para muestras reales, los LOD se suelen considerar 100 veces superiores.....	96
Tabla 2.2. Parámetros instrumentales para los diferentes ICP-OES empleados.....	99
Tabla 2.3. Longitudes de onda y principales interferencias observadas para los elementos analizados empleando los distintos ICP-OES.....	101
Tabla 2.4. Condiciones instrumentales de operación del ICP-MS ThermoElemental Pq ExCell.....	103
Tabla 2.5. Sumario de masas empleadas e interferencias poliatómicas e isobáricas observadas.....	104
Tabla 2.6. Parámetros instrumentales de medida por fluorescencia de rayos-X.....	105
Tabla 2.7. Condiciones experimentales empleadas en el tratamiento de muestras llevando a cabo las extracciones secuenciales mediante los distintos equipos de ultrasonidos.....	110
Tabla 2.8. Contenidos totales de metales pesados ($\text{mg} \cdot \text{kg}^{-1}$) de los diferentes CRMs empleados a lo largo de este estudio.....	127
Tabla 2.9. Composición de los distintos CRMs empleados a lo largo de este estudio.....	127
Tabla 2.10 Clasificación de los suelos en función de su acidez.....	129
Tabla 2.11. Clasificación del tipo de suelo en función del contenido de sales disueltas, expresado como conductividad.....	130

Capítulo 3. Validación de Métodos Analíticos

FIGURAS

Figura 3.1. Clasificación jerárquica de referencias según la importancia metrológica o nivel de trazabilidad. A) Métodos y materiales de referencia primarios. B) Métodos y materiales de referencia secundarios. C) Materiales de referencia de trabajo.....	142
Figura 3.2. Influencia del pH del extractante en la extracción de metales durante la segunda etapa del BCR-SES aplicado sobre el BCR 601.....	158
Figura 3.3. Comparativa de la fraccionación convencional de Cd, Cr, Cu, Ni, Pb y Zn en el BCR 601 y 701, empleando el SM&T-SES convencional (Conv) con respecto a las variantes aceleradas de dicho proceso empleando la metodología monoetapa (Mono) o la de sonda de ultrasonidos (US).....	172
Figura 3.4. Mapas de contorno para la optimización de la pseudodigestión de Cd y Cr en el CRM BCR 141R siguiendo la variación del % de recuperación en función de las variables tiempo, temperatura y relación volumen:sólido.....	178
Figura 3.5. Mapas de contorno para la optimización de la pseudodigestión de Cu y Ni en el CRM BCR 141R siguiendo la variación del % de recuperación en función de las variables tiempo, temperatura y relación volumen: sólido.....	179
Figura 3.6. Mapas de contorno para la optimización de la pseudodigestión de Pb y Zn en el CRM BCR 141R siguiendo la variación del % de recuperación en función de las variables tiempo, temperatura y relación volumen: sólido.....	180

TABLAS

Tabla 3.1. Límites de detección y cuantificación de los distintos elementos determinados en los extractos de los SES, extracciones simples y pseudodigestión mediante ICP-OES ($\mu\text{g} \cdot \text{g}^{-1}$).....	148
--	-----

Tabla 3.2. Límites de detección y cuantificación de los distintos elementos determinados en los extractos de los SES, extracciones simples y pseudodigestión mediante ICP-MS (ng g ⁻¹).	149
Tabla 3.3. Curvas de calibrado y comparación de pendientes de calibración para la determinación de metales en extractos o pseudodigestiones empleando ICP-OES. Diferencias significativas sombreadas y en cursiva (>5%). El coeficiente de correlación de los diferentes elementos en los distintos extractos o pseudodigestiones fue > 0.999.	151
Tabla 3.4. Curvas de calibrado y comparación de pendientes de calibración para la determinación de metales en extractos o pseudodigestiones empleando ICP-MS. Diferencias significativas sombreadas y en cursiva (>5%). El coeficiente de correlación de los diferentes elementos en los distintos extractos o pseudodigestiones fue > 0.999.	152
Tabla 3.5. Resultados para la fracción soluble en ácido para el BCR 601 y el BCR 701 empleando el SM&T-SES y el BCR-SES. n=8. Recuperación (% R). Los valores certificados o indicativos van acompañados de la incertidumbre total expandida asociada mientras que el valor experimental presenta el intervalo de confianza asociado. <i>El valor de Cu en el BCR-SES no se encuentra certificado, es indicativo dada la inestabilidad observada para este elemento durante la certificación del CRM.</i>	155
Tabla 3.6. Resultados para la fracción reducible empleando el SM&T-SES y el BCR-SES para el BCR 601 y el BCR 701 n=8. Recuperación (% R). Los valores certificados o indicativos van acompañados de la incertidumbre total expandida asociada mientras que el valor experimental presenta el intervalo de confianza asociado. <i>No se proporcionan valores certificados de Cr y Cu para el BCR-SES normal o a largo plazo. El valor de Pb para el BCR-SES es indicativo.</i>	157
Tabla 3.7. Resultados para la fracción oxidable obtenidos tras la aplicación del SM&T-SES y BCR-SES sobre el BCR 601 y el BCR 701. n=8. Recuperación (%R). Los valores certificados o indicativos van acompañados de la incertidumbre total expandida asociada mientras que el valor experimental presenta el intervalo de confianza asociado. <i>No se proporcionan valores certificados de Cr, Cu y Zn para el BCR 601 empleando el BCR-SES.</i>	160
Tabla 3.8. Resultados para la fracción reducible empleando el BCR-SES y el SM&T-SES acelerado por procesos monoetapa para los BCR 601 y 701. n=4. Recuperación (R%). Los valores certificados o indicativos van acompañados de la incertidumbre total expandida asociada mientras que el valor experimental presenta el intervalo de confianza asociado.	163
Tabla 3.9. Resultados para la fracción oxidable empleando el BCR-SES y el SM&T-SES acelerado por procesos monoetapa para los BCR 601 y 701. n=4. Recuperación (%R). Los valores certificados o indicativos van acompañados de la incertidumbre total expandida asociada mientras que el valor experimental presenta el intervalo de confianza asociado.	164
Tabla 3.10. Concentraciones de metales [mg kg ⁻¹] extraídas en función del tiempo de sonicación para el SM&T-SES acelerado por baño de ultrasonidos aplicado sobre el BCR 601. n=4. Recuperación (%R).	166
Tabla 3.11. Resultados para la fracción soluble en ácido empleando el SM&T-SES acelerado por sonda de ultrasonidos para los BCR 601 y 701. n=4. Recuperación (%R). Los valores certificados o indicativos van acompañados de la incertidumbre total expandida asociada mientras que el valor experimental presenta el intervalo de confianza asociado.	167
Tabla 3.12. Resultados para la fracción reducible empleando el SM&T-SES acelerado por sonda de ultrasonidos para los BCR 601 y 701. n=4. Recuperación (%R). Los valores certificados o indicativos van acompañados de la incertidumbre total expandida asociada mientras que el valor experimental presenta el intervalo de confianza asociado.	168
Tabla 3.13. Resultados para la fracción oxidable empleando el SM&T-SES acelerado por sonda ultrasonidos para los BCR 601 y 701. n=4. Recuperación (%R). Los valores certificados o indicativos van acompañados de la incertidumbre total expandida asociada mientras que el valor experimental presenta el intervalo de confianza asociado.	169
Tabla 3.14. Resumen del contenido total extraíble [Σ F1,F2,F3] (mg kg ⁻¹) para el BCR 701 y 601 por el proceso convencional y las versiones aceleradas del SM&T-SES. La recuperación (% R) se calcula como la relación entre el contenido extraído utilizando el proceso acelerado y el contenido extraído utilizando el proceso convencional.	171
Tabla 3.15. Aplicación del método de reflujo a los CRMs, BCR 141R y BCR 601, para n=4. Los valores certificados van acompañados por la incertidumbre total expandida asociada mientras que los valores experimentales presentan el intervalo de confianza asociado.	173
Tabla 3.16. Comparación de los resultados obtenidos siguiendo el protocolo de extracción secuencial del SM&T-SES y el protocolo de extracción con agua regia mediante el método de reflujo para el BCR 141R y 601. [mg kg ⁻¹].	174
Tabla 3.17. Resumen de los niveles de los factores empleados en el diseño de experimentos para la pseudodigestión de muestras con matriz geológica (CRM BCR 141R).	176

Tabla 3.18. Condiciones optimizadas para la pseudodigestión de muestras geológicas empleando el microondas analítico y relaciones volumen:sólido de 40 o 70 ml g ⁻¹	181
Tabla 3.19. Aplicación del método de pseudodigestión acelerado por microondas a los CRMs, BCR 141R y BCR 601, para n=4, priorizando el gasto de reactivos (40 ml g ⁻¹). Recuperación (%R). Los valores certificados van acompañados por la incertidumbre total expandida asociada mientras que los valores experimentales presentan el intervalo de confianza asociado.	182
Tabla 3.20. Comparación de los resultados obtenidos siguiendo el protocolo de extracción secuencial del SM&T-SES y el protocolo de extracción con agua regia mediante el método optimizado de pseudodigestión acelerado por microondas para los BCR 141R y 601. [mg kg ⁻¹].....	183
Tabla 3.21. Comparativa de los errores relativos del proceso de pseudodigestión por reflujos o pseudodigestión acelerada por microondas para el BCR 141R y el BCR 601.	184
Tabla 3.22. Resultados de la extracción simple con HAcO 0.43 mol L ⁻¹ sobre el CRM BCR 483, para n=6. Todos los valores certificados se acompañan por la incertidumbre total expandida asociada.	185
Tabla 3.23. Resultados de la extracción simple con EDTA 0.05 mol L ⁻¹ sobre el CRM BCR 483, para n=6. Todos los valores certificados se acompañan por la incertidumbre total expandida asociada.	186
Tabla 3.24. Resultados de la extracción simple con CaCl ₂ 0.01 mol L ⁻¹ sobre el CRM BCR 483, para n=6. En este caso el valor indicativo proporcionado viene acompañado por la desviación estándar.....	186
Tabla 3.25. Resultados de la extracción simple con NaNO ₃ 0.05 mol L ⁻¹ sobre el CRM BCR 483, para n=6. En este caso el valor indicativo proporcionado viene acompañado por la desviación estándar.....	187

Capítulo 4. Aplicaciones de los SES. Análisis multivariable y geoestadística.

FIGURAS

Figura 4.1. Localización geográfica del asentamiento minero de Salsigne en la región del Aude. (Francia).	199
Figura 4.2. Localización de los 21 puntos de muestreo dentro del área estudiada de la mina de Salsigne.	200
Figura 4.3. Patrón de fraccionamiento de As para los diferentes puntos de muestreo con respecto al contenido pseudototal (mg kg ⁻¹) y expresado en porcentaje de la cantidad total.....	211
Figura 4.4. Patrón de fraccionamiento de Cd para los diferentes puntos de muestreo con respecto al contenido pseudototal (mg kg ⁻¹) y expresado en porcentaje de la cantidad total.	213
Figura 4.5. Patrón de fraccionamiento de Cu para los diferentes puntos de muestreo con respecto al contenido pseudototal (mg kg ⁻¹) y expresado en porcentaje de la cantidad total.	214
Figura 4.6. Patrón de fraccionamiento de Ni para los diferentes puntos de muestreo con respecto al contenido pseudototal (mg kg ⁻¹) y expresado en porcentaje de la cantidad total.	215
Figura 4.7. Patrón de fraccionamiento de Pb para los diferentes puntos de muestreo con respecto al contenido pseudototal (mg kg ⁻¹) y expresado en porcentaje de la cantidad total.	216
Figura 4.8. Patrón de fraccionamiento de Zn para los diferentes puntos de muestreo con respecto al contenido pseudototal (mg kg ⁻¹) y expresado en porcentaje de la cantidad total.....	217
Figura 4.9. Porcentajes de labilidad de Cd, Cu y Pb en las muestras de suelos y sedimentos contaminados de Salsigne.	219
Figura 4.10. Porcentajes de labilidad de As, Ni y Zn en las muestras de suelos y sedimentos contaminados de Salsigne.	219
Figura 4.11. Representación de scores y loadings para el PCA del contenido de las pseudodigestiones sobre las 21 muestras de Salsigne. PC ₁ (Primer componente principal), PC ₂ (Segundo componente principal).....	225
Figura 4.12. Representación del dendograma resultante del HCA empleando los scores obtenidos en el PCA de los contenidos pseudototales de las muestras de Salsigne. Se emplea el método de agrupación de Ward y la distancia Euclidiana al cuadrado como medida de similitud.	225
Figura 4.13. Representación de scores y loadings para el PCA del contenido de las extracciones con ácido acético 0,11 mol L ⁻¹ , sobre las 21 muestras de Salsigne. PC ₁ (Primer componente principal), PC ₂ (Segundo componente principal).....	227
Figura 4.14. Representación del dendograma resultante del HCA empleando los scores obtenidos en el PCA de los contenidos extraídos en la fracción soluble en ácido de las muestras de Salsigne. Se emplea el método de agrupación de Ward y la distancia Euclidiana al cuadrado como medida de similitud.....	227
Figura 4.15. Representación de scores y loadings para el PCA del contenido de las extracciones con cloruro de hidroxilamina 0,5 mol L ⁻¹ , sobre las 21 muestras de Salsigne. PC ₁ (Primer componente principal), PC ₂ (Segundo componente principal).....	229
Figura 4.16. Representación del dendograma resultante del HCA empleando los scores obtenidos en el PCA de los contenidos extraídos en la fracción reducible de las muestras de Salsigne. Se emplea el método de agrupación de Ward y la distancia Euclidiana al cuadrado como medida de similitud.....	229

Figura 4.17. Representación de scores y loadings para el PCA del contenido de las extracciones con peróxido de hidrógeno y acetato de amonio $1,0 \text{ mol}\cdot\text{L}^{-1}$, sobre las 21 muestras de Salsigne. PC_1 (Primer componente principal), PC_2 (Segundo componente principal).....231

Figura 4.18. Representación del dendograma resultante del HCA empleando los scores obtenidos en el PCA de los contenidos extraídos en la fracción oxidable de las muestras de Salsigne. Se emplea el método de agrupación de Ward y la distancia Euclidiana al cuadrado como medida de similitud.232

Figura 4.19. Scores para los resultados de F1, F2, F3 y F4 en función del punto de muestreo para el primer componente principal de los correspondientes PCAs.233

Figura 4.20. Patrones de fraccionación promedio para As, Cd, Cu, Ni, Pb y Zn pertenecientes a los diferentes grupos de muestras derivados del análisis estadístico multivariable de los datos. a.) Grupo I. b.) Grupo II. c.) Grupo III.....235

Figura 4.21. Variograma omnidireccional y parámetros estimados asociados para los datos de la extracción de As en la fracción soluble en ácido ajustados a un modelo esférico.239

Figura 4.22. Mapas de distribución espacial de la contaminación de As en las diferentes fracciones del SES-SM&T empleando métodos geoestadísticos, siguiendo los modelos recogidos en la Tabla 4.7244

Figura 4.23. Mapas de distribución espacial de la contaminación de Cd en las diferentes fracciones del SES-SM&T empleando métodos geoestadísticos, siguiendo los modelos recogidos en la Tabla 4.7.245

Figura 4.24. Mapas de distribución espacial de la contaminación de Cu en las diferentes fracciones del SES-SM&T empleando métodos geoestadísticos, siguiendo los modelos recogidos en la Tabla 4.7.246

Figura 4.25. Mapas de distribución espacial de la contaminación de Ni en las diferentes fracciones del SES-SM&T empleando métodos geoestadísticos, siguiendo los modelos expuestos en la Tabla 4.7.247

Figura 4.26. Mapas de distribución espacial de la contaminación de Pb en las diferentes fracciones del SES-SM&T empleando métodos geoestadísticos, siguiendo los modelos recogidos en la Tabla 4.7.248

Figura 4.27. Mapas de distribución espacial de la contaminación de Zn en las diferentes fracciones del SES-SM&T empleando métodos geoestadísticos, siguiendo los modelos recogidos en la Tabla 4.7.249

TABLAS

Tabla 4.1. Sumario de las características edafológicas de las muestras de suelos y sedimentos de Salsigne.201

Tabla 4.2. Contenido pseudototal de metales en las muestras de suelos y sedimentos del asentamiento minero de Salsigne. ($\text{mg}\cdot\text{kg}^{-1}$).....203

Tabla 4.3. Rangos de concentración, valores típicos observados en suelos, abundancia media en la corteza terrestre, niveles legislativos holandeses y franceses de As, Cd, Cu, Ni Pb y Zn en suelos contaminados. ($\text{mg}\cdot\text{kg}^{-1}$).¹.....204

Tabla 4.4. Componentes mayoritarios de las muestras de suelos y sedimentos del área de Salsigne, expresados con respecto al % de materia seca (n=2).206

Tabla 4.5. Contenido de metales en las diferentes fracciones del SM&T-SES de las muestras de suelos y sedimento del área de Salsigne. ($\text{mg}\cdot\text{kg}^{-1}$). F1) Fracción soluble en ácido. F2) Fracción reducible. F3) Fracción oxidable. F4) Fracción residual.....207

Tabla 4.6. Asimetría, amplitud y nivel de significación para el test de normalidad de Kolmogorov-Smirnov de los datos originales, transformados logarítmicamente y transformados por Box-Cox de los datos de las extracciones de las muestras de Salsigne. *Sombreados y en cursiva, variables para las que el valor de la distancia de Kolmogorov-Smirnov (K-S d) obtenido falla el test estadístico al proporcionar un valor de $p < \alpha=0,05$.*.....222

Tabla 4.7. Modelos ajustados y parámetros asociados a los variogramas experimentales de los datos de las variables transformadas de los distintos metales en las diferentes fracciones del SM&T-SES.238

Capítulo 5. SES aplicados a sedimentos depositados en arcén de autopista

FIGURAS

Figura 5.1. Distribución y vías de difusión de la contaminación antropogénica asociada al tráfico.....259

Figura 5.2. Densidad de las vías de circulación en las proximidades del área metropolitana de Barcelona.....264

Figura 5.3. Localización del área muestreada de la autopista C-58 en las inmediaciones del área metropolitana de Barcelona.265

Figura 5.4. Valores de concentración pseudototal de Cd, Cr y Ni, normalizados con respecto al valor objetivo de la legislación holandesa para las muestras de la autopista C-58 ordenadas en función del punto de muestreo desde Viladecavalls (M9) hasta Barcelona (M8).277

Figura 5.5. Valores de concentración pseudototal de Cu, Pb y Zn, normalizados con respecto al valor objetivo de la legislación holandesa para las muestras de la autopista C-58 ordenadas en función del punto de muestreo desde Viladecavalls (M9) hasta Barcelona (M8).277

Figura 5.6. Factores de enriquecimiento para diferentes elementos estimados en el análisis del contenido pseudototal de las muestras de sedimento de la autopista C-58.	280
Figura 5.7. Patrón de fraccionamiento de Al para los diferentes puntos de muestreo con respecto al contenido pseudototal (mg·kg ⁻¹) y expresado en porcentaje de la cantidad total.	284
Figura 5.8. Patrón de fraccionamiento de Cd para los diferentes puntos de muestreo con respecto al contenido pseudototal (mg·kg ⁻¹) y expresado en porcentaje de la cantidad total.	285
Figura 5.9. Patrón de fraccionamiento de Cr para los diferentes puntos de muestreo con respecto al contenido pseudototal (mg·kg ⁻¹) y expresado en porcentaje de la cantidad total.	286
Figura 5.10. Patrón de fraccionamiento de Cu para los diferentes puntos de muestreo con respecto al contenido pseudototal (mg·kg ⁻¹) y expresado en porcentaje de la cantidad total.	288
Figura 5.11. Patrón de fraccionamiento de Ni para los diferentes puntos de muestreo con respecto al contenido pseudototal (mg·kg ⁻¹) y expresado en porcentaje de la cantidad total.	289
Figura 5.12. Patrón de fraccionamiento de Pb para los diferentes puntos de muestreo con respecto al contenido pseudototal (mg·kg ⁻¹) y expresado en porcentaje de la cantidad total.	291
Figura 5.13. Patrón de fraccionamiento de Zn para los diferentes puntos de muestreo con respecto al contenido pseudototal (mg·kg ⁻¹) y expresado en porcentaje de la cantidad total.	292
Figura 5.14. Valores medioambientales guía para las diferentes fracciones de los SES para los elementos más favorecidos antropogénicamente y normalizados con respecto al valor objetivo de la legislación holandesa. La línea continua representa el valor objetivo y la discontinua el valor de intervención.	294
Figura 5.15. Comparativa de los factores de enriquecimiento promedio obtenidos en cada fracción del SM&T-SES para los elementos contaminantes en estudio.	295
Figura 5.16. Porcentajes de labilidad de Cd, Cr, Cu, Ni, Pb y Zn en función del contenido total movilizable ([F1+F2+F3]) expresado en mg·kg ⁻¹	297
Figura 5.17. Comparativa de porcentajes de labilidad de Cu, Pb y Zn en los sedimentos de la autopista C-58 con respecto a los observados en otros estudios, representados en azul. ^{26,50,52,56,-}	299
Figura 5.18. Promedio de los cocientes de extracción para Cd, Cr, Cu, Ni, Pb y Zn en función de los extractantes ácidos empleados en las extracciones simples.	301
Figura 5.19. Promedio del cociente de extracción para Cd, Cr, Cu, Ni, Pb y Zn, comparando procesos de complejación y acidificación.	304
Figura 5.20. Representación del promedio de la movilidad a largo plazo [MOB] (mg·kg ⁻¹) y el promedio del índice de movilidad [iMOB] para Cd, Cr, Cu, Ni, Pb y Zn, en las muestras de sedimentos de la autopista C-58.	306
Figura 5.21. Representación de los porcentajes de recuperación de Al con respecto al contenido pseudototal en los distintos extractantes empleados. El eje X se encuentra en escala logarítmica.	308
Figura 5.22. Recuperación media relativa a los contenidos pseudototales de Cd, Cr, Cu, Ni, Pb y Zn en función de los extractantes empleados. El eje de las X se encuentra en escala log ₁₀	311
Figura 5.23. Representación de la correlación existente entre las concentraciones de los metales favorecidos antropogénicamente en las muestras de la C-58 para los extractos de HCl y la suma de los contenidos movilizables.	314

TABLAS

Tabla 5.1. Sumario de aportaciones contaminantes a sedimentos depositados sobre pavimento asfáltico (carreteras, autopistas, etc...).	261
Tabla 5.2. Índice calculado de emisión de metales pesados asociados al tráfico rodado y clasificados en función de la fuente de emisión (Ton/año, 2002).	262
Tabla 5.3. Descripción de los puntos de muestreo seleccionados a lo largo de la autopista C58.	265
Tabla 5.4. Parámetros edafológicos de las muestras de sedimentos de la autopista C-58 (M) y en las muestras de nivel de fondo (B).	267
Tabla 5.5. Contenido pseudototal de metales en la muestras de los sedimentos depositados en la C-58 (M) y en las muestras de nivel de fondo (B), (mg·kg ⁻¹), excepto Al (g·kg ⁻¹).	269
Tabla 5.6. Componentes mayoritarios de los sedimentos depositados junto a la calzada de la autopista C-58, así como las muestras de nivel de fondo, expresados con respecto al % de materia seca. n=2.	272
Tabla 5.7. Balance de masas relacionado con el aporte de Zn a los sedimentos de la C-58 considerando la degradación de los neumáticos.	273
Tabla 5.8. Balance de masas relacionado con el aporte de Pb a los sedimentos de la C-58 considerando las emisiones producidas por los vehículos que consumen gasolina.	274
Tabla 5.9. Sumario estadístico del contenido pseudototal, valores de los CERs, valores guía de concentración (ECG) y el número de muestras por clase de CER para Cd, Cr, Cu, Ni, Pb y Zn en 13 muestras de sedimentos depositados en la autopista C-58.	276
Tabla 5.10. Significado de los valores de los factores de enriquecimiento.	278

Tabla 5.11. Contenido de metales en las diferentes fracciones del SES de las muestras de sedimento de la C-58. (mg kg ⁻¹). F1) Fracción soluble en ácido. F2) Fracción reducible. F3) Fracción oxidable. F4) Fracción residual.	281
Tabla 5.12. Resumen de concentraciones medias, máximas y mínimas de metales extraíbles utilizando extracciones simples en las muestras de sedimento de la autopista C-58 y en las muestras de nivel de fondo. (RDS, sedimento depositado). (Bkgrd, Muestras de nivel de fondo).	302
Tabla 5.13. Movilidad a largo plazo de los diferentes metales contaminantes en las muestras de sedimentos de la autopista C58. Valores en mg kg ⁻¹ , excepto Cd y Cr, en µg kg ⁻¹	305
Tabla 5.14. Correlaciones de Spearman entre las recuperaciones de 6 metales y el contenido de carbonatos en los diferentes extractantes empleados para las 13 muestras de sedimentos.	309
Tabla 5.15. Coeficientes de correlación de Spearman para las cantidades liberadas de los elementos favorecidos antropogénicamente empleando diferentes extractantes.	313

Capítulo 6. Estudios de readsorción y redistribución

FIGURAS

Figura 6.1. Fraccionación de los distintos CRMs empleando el BCR-SES. BCR 483 (483), BCR 601 (601), BCR 701 (701).	331
Figura 6.2. Comparativa de los patrones de fraccionación de distintos CRMs, aplicando el SM&T-SES.	344
Figura 6.3. Redistribución de las cantidades reabsorbidas en la primera etapa (F1) del SM&T-SES para los CRMs estudiados.	353
Figura 6.4. Redistribución de las cantidades reabsorbidas en la segunda etapa (F2) del SM&T-SES para los CRMs estudiados.	354
Figura 6.5. Comparativa de los patrones de fraccionación de distintos CRMs, aplicando el SM&T-SES sin considerar (izquierda) y considerando (derecha) las correcciones introducidas en función de las cantidades reabsorbidas y redistribuidas.	356

TABLAS

Tabla 6.1. Fraccionación de los distintos CRMs empleados [mg kg ⁻¹] para evaluar la readsorción empleando el BCR-SES. Los resultados experimentales se expresan como media ± intervalo de confianza. n=8, excepto BCR 483 n=4.	331
Tabla 6.2. Cantidades añadidas [M(µg)] y porcentajes de readsorción [Read(%)] (expresados como media ± intervalo de confianza) de los diferentes metales, en los distintos CRMs empleados, al evaluar la readsorción en el BCR-SES. n=3.	333
Tabla 6.3. Fraccionación de los distintos CRMs empleados para evaluar la readsorción empleando el BCR-SES acelerado por procesos monoetapa. Resultados expresados como media ± intervalo de confianza. [mg kg ⁻¹]. n=4.	337
Tabla 6.4. Cantidades añadidas (µg) y porcentajes de readsorción (%) de los diferentes metales en los distintos CRMs al aplicar el BCR-SES convencional (Conv) y la variante acelerada por procesos monoetapa (Mono). Resultados expresados como media ± intervalo de confianza. n=3.	339
Tabla 6.5. Fraccionación de los distintos CRMs empleados para evaluar la readsorción y redistribución empleando el SM&T-SES. [mg kg ⁻¹]. n=4, excepto BCR 601 y 701, para los que n=8. Los resultados se expresan como media ± intervalo de confianza.	342
Tabla 6.6. Valores bibliográficos de la fraccionación del BCR 483 y el SRM 2710 para efectuar la comparativa con respecto a la fraccionación obtenida en el presente estudio.	343
Tabla 6.7. Cantidades añadidas M(µg) y porcentajes de readsorción de los diferentes metales en los distintos CRMs al aplicar el SM&T-SES. Sombreados y en cursiva, aquellos CRMs que carecen de resultados indicativos o certificados para evaluar la validez de la fraccionación convencional. Los resultados se expresan como media ± intervalo de confianza. n=3.	347
Tabla 6.8. Cantidades añadidas M(µg) y porcentajes de readsorción Read(%) de los diferentes metales en los distintos CRMs al aplicar el SM&T-SES en los estudios de redistribución. Sombreados, aquellos CRMs que carecen de resultados indicativos o certificados para evaluar la validez de la fraccionación convencional. Los resultados se expresan como media ± intervalo de confianza. n=3.	348
Tabla 6.9. Fraccionación de los distintos CRMs empleados para evaluar la readsorción empleando el SM&T-SES acelerado por procesos monoetapa y por ultrasonidos. [mg kg ⁻¹]. n=4. Los resultados se expresan como media ± intervalo de confianza.	358
Tabla 6.10. Resumen comparativo de la readsorción en las distintas fracciones del SM&T-SES sobre distintos CRMs empleando la versión convencional (Conv) y la versión acelerada por procesos monoetapa (Mono). Los resultados se expresan como media ± intervalo de confianza. n=3.	362

Tabla 6.11. Resumen comparativo de la readsorción en las distintas fracciones del SM&T-SES sobre distintos CRMs empleando la versión convencional (Conv) y la versión acelerada por ultrasonidos (US). Los resultados se expresan como media \pm intervalo de confianza. n=3.	364
Tabla 6.12. Sumario de los resultados (concentraciones) derivadas de la fraccionación de las muestras del área minera de Salsigne empleando el SM&T-SES convencional y la variante acelerada por procesos monoetapa. (mg kg ⁻¹).....	366
Tabla 6.13. Composición mayoritaria de las muestras (procedente de la tabla 4.4).....	367
Tabla 6.14. Cantidades añadidas M(μ g) y porcentaje de readsorción Read(%) para los distintos elementos en diferentes muestras de suelos contaminados al aplicar el SM&T-SES, en la variante convencional (Conv) y en la variante acelerada por procesos monoetapa (Mono). En cursiva y sombreados aquellos elementos para los que se observaron diferencias significativas entre la fraccionación convencional y acelerada al estudiar la readsorción empleando CRMs. Los resultados se expresan como media \pm intervalo de confianza. n=3).....	369

ANEXO 3

Determination of pollution trends in an abandoned mining site by application of a multivariate statistical analysis to heavy metals fractionation using SMGT-SES.

G. Pérez, M. Valiente. *Journal of Environmental Monitoring*. 2005, 7, 29-36.

Determination of pollution trends in an abandoned mining site by application of a multivariate statistical analysis to heavy metals fractionation using SM&T-SES†

G. Pérez and M. Valiente*

Centre GTS, Unitat de Química Analítica, Departament de Química, Universitat Autònoma de Barcelona, Facultat de Ciències, Edifici CN, 08193, Bellaterra, Barcelona, Spain.
E-mail: Manuel.Valiente@uab.es

Received 23rd July 2004, Accepted 10th November 2004

First published as an Advance Article on the web 3rd December 2004

The mobility, availability and persistence of Heavy Metals (HMs), As, Cd, Cu, Ni, Pb and Zn, in contaminated soils of a former abandoned mining area were evaluated by means of a sequential extraction scheme (SES) and applying a multivariate statistical analysis to the obtained data. Chemical partitioning of HMs in each sample was determined in four fractions (acid-soluble, reducible, oxidable and residual) following the Standard Measurements and Testing (SM&T) SES, formerly BCR-SES. Statistical evaluation of results by pattern recognition techniques allowed identification of groups of samples with similar characteristics and observations of correlations between variables, determining the pollution trends and distribution of HMs within the studied area. Typical metal-fraction association and metal availability characteristics of heavy metals have been depicted. The obtained results indicate an urgent need to attenuate the hazard in that area posed by high concentrations of toxic metals, which exceed the limits specified by different European legislations on soil reclamation.

Introduction

Different pollution sources that have been topics of recent interest include improper waste dumping, incidental accumulation, agricultural chemicals, abandoned industrial activities and atmospheric fallout, among the most cited.¹ In particular, for mining and industrial abandoned sites, prior to evaluating the recovery of the polluted area, an evaluation of the extent and distribution of contamination is required in order to identify the area to be treated and the type of treatment that should be considered based upon the observed pollution trends. In these sources, heavy metals, HMs, frequently are the main pollutants and their mobilization due to weathering of solid inorganic materials under exogenic conditions is favoured, leading to environmental chemical pollution.

For risk assessment purposes, the HMs mobility and their related availability is of a primal importance since toxicity is directly related to such characteristics.² Moreover, as is well known, pseudototal HMs content does not provide real information on available amounts of HMs and it represents the worst possible situation, overestimating the real hazard. Consequently, there is a need for a methodology able to provide information about reactivity or mobility of pollutants. In this sense, sequential extraction schemes (SES), became a commonly used evaluative and informative tool by providing details on the distribution or partitioning of HMs in soils and sediments, which is directly related to the prediction of their mobility.¹

This methodology is based on the process known as fractionation,³ where a sequential series of selective extractant reagents with an increasing extractant power is employed. The goal of this procedure is to selectively dissolve or solubilise the different solid phases or mineralogical fractions.⁴⁻⁶ By this methodology, knowledge of how HMs partition among the various geochemical phases is obtained. Such knowledge allows for a better insight into the mechanisms of HMs retention and

release involved in the process of migration and decontamination, thus providing an evaluation of availability, mobility or persistence.

Two decades ago, Tessier proposed a five-step SES, which is still widely used,⁷ often with modifications in order to fit better to the target sample.^{8,9} SES have been widely used to assess the mobile fraction of different HMs of environmental impact and to evaluate the HMs distribution between the different phases of a variety of samples such as industrially contaminated soils,¹⁰⁻¹⁹ river sediments,²⁰⁻²⁵ sewage sludge,²⁶⁻³⁰ etc. The wide variety of SES and the related lack of comparability between results, led to the harmonisation of SES under the auspices of the former Community Bureau of Reference (BCR), now Standards Measurements and Testing (SM&T), producing a certified reference material for a three-step SES.³¹⁻³³

The main drawbacks of SES have been identified as readorption and redistribution of metals.³⁴⁻³⁷ Also, SES applications have been mostly limited to low contamination sites. However, SES are still very useful to identify trace element partitioning into the various solid phases of soil and to determine labile fractions of trace elements in a verifiable manner. On the other hand, SES data can provide additional valuable knowledge by a proper exploratory data analysis of the experimental information. For instance, a systematic correlation of the different fractionation data, normally absent, would help the process characterization of a particular contaminated area.

Taking into account the mentioned limitations, the present study has been addressed to reveal the potential of SES application to a highly polluted site in overcoming the indicated boundaries. In this context, the present investigation is concerned with the fractionation of the HMs As, Cd, Cu, Ni, Pb and Zn in soils of a ditch network system designed to confine, control and monitor flows of water at a former abandoned mining area at Salsigne (France). Although As has not been considered in the SM&T-SES reference materials and applications (except in a recent work),³⁸ we have analysed the As content in the different target fractions because it is the main toxic contaminant of the target soils. We are aware of the

† Electronic supplementary information (ESI) available: complete HMs fractionation dataset. See <http://www.rsc.org/suppdata/em/b4/b411316k/>

limitations of such results on As for a possible contribution to risk evaluation due to its particular chemical behaviour as an oxoanion. In this sense, values can be taken as the minimum mobility of this element under the given conditions. Furthermore, to best characterize the polluted site, a correlation of sample content was carried out by multivariate statistical analysis of SES data including latent factors responsible for the data set structure and apportioning of pollutant sources. A comparison of the obtained data with current regulation limits has been carried out and can be of use for risk assessment purposes.

Experimental

Sampling site

The polluted site of Salsigne is located in southern France, in the Orbiel river basin, 13 km north of Carcassonne. Geologically, the site mainly includes accumulations of sulfide minerals containing various metals such as iron, copper, gold, as well as arsenic and bismuth. Large surfaces present a significant pollution problem due to improper waste storage, although it is difficult to complete a related inventory because important masses of waste are not visible. Pollution of the locations around the treatment installations and waste storage areas is very high and is also important under these installations due to the percolation of pollutants in the ground. Broader pollution has been driven by rainwater leaching of pollutants, which flow into the Orbiel River and to some of its effluents. Appropriate measurements of pollutants are essential to assess suitable actions and thus prevent serious harmful problems. Because of the frequent strong winds in this area, additional pollution is produced from dust emitted to the atmosphere by the old pyrometallurgical installations or take-offs from deposits of very fine residues of arsenic oxides. Currently, there are approximately 5000 tons of these wastes, but demolition of buildings around furnaces will probably uncover a few hundred additional tons. The total contaminated zone covers an estimated area of 40 hectares.

Fig. 1 presents the locations of single sampling points within the studied area. The sampling points were selected in a random manner to cover both the whole ditches network, which displays varying degrees of pollution, and relevant locations within the polluted area. A total of 21 surface samples were collected. 11 samples were collected along the ditches network and 10 from polluted surfaces exposed to significant flow of water during rain events, close to ditches.

Sample preparation and soil properties

Composite samples were made of 10 unit samples mixed together to provide a better representation of a selected surface

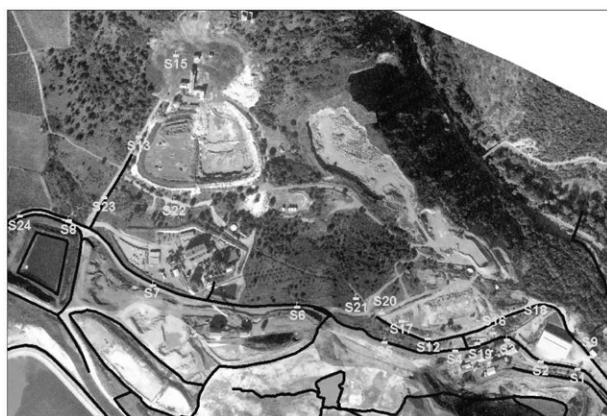


Fig. 1 Location of sampling points on the polluted site of Salsigne. Black lines represent the ditches network.

by obtaining the composition average. Surface unit samples (10 cm) were collected with a trowel (after removing the top 2 cm layer in contact with the atmosphere). Soil samples were air dried and ground to below 100 μm grain size with a tungsten steel bite grinder, which was cleaned with inert material between samples. Such a particle size was selected to accomplish a similarity with the employed CRM (BCR 701) to assess the traceability of the applied SM&T-SES. Once prepared, samples were placed in plastic bags or polypropylene bottles and stored at 4 $^{\circ}\text{C}$ to prevent possible changes in metal fractionation. Soil characteristics, hereafter called edaphological parameters, such as pH (total and potential), conductivity and organic matter content, were determined according to the official methods of soil analysis envisaged by local governmental regulations (Junta de Residus, Generalitat de Catalunya).³⁹ Total and potential soil pH were determined in a soil : water (1.0 : 2.5) and soil : KCl 0.1 mol^{-1} (1.0 : 2.5) ratio suspension, respectively, at room temperature. Organic matter was evaluated by loss on ignition at 600 $^{\circ}\text{C}$ after 4 h. Conductivity was evaluated after extracting a soil : water (1 : 10) ratio suspension for 2 h. Major components were determined by X-ray fluorescence spectrometry (XRF) using 56 geological international reference samples for calibration. Samples were diluted (1 : 40) with lithium tetraborate and melted in a radio-frequency inductive oven to obtain 30 mm diameter pearls. Ranges and average values of sample characteristics are given in Table 1.

Procedure for sequential extraction

The applied SES corresponds to the Standard Measurements and Testing procedure (SM&T-SES), including the updated modifications to improve the reproducibility of results.⁴⁰ The corresponding four fractions, including the recommended pseudototal digestion of the remaining residue (F4) after the three steps of the SM&T-SES, are described in Table 2. Microwave digestion treatment was applied to determine both pseudototal metal determination in the original samples and residual fraction (F4). For quality control, a mass balance was evaluated by comparison of the pseudototal metal content determined in the original samples with the sum of extracted metal percentages in the four steps. Prior to application to real samples, the SM&T-SES was validated by means of the BCR 701 reference material, obtaining a good traceability for corresponding HMs in each fraction as can be deduced from Table 3. After each SES step, the suspension was centrifuged and the supernatant separated from the solid phase by filtering through a 0.22-micron filter Millex-GS (Millipore, Ireland) to avoid the

Table 1 Edaphological parameters and major components for 11 samples collected from the ditches network and 10 samples collected from polluted surfaces with significant flow of water after rain events at the polluted site of Salsigne and subjected to the SM&T-SES

	Range	Mean
pH (potential/total)	6.4–8.6/5.3–7.9	7.6/7.2
Organic matter (%)	0.01–0.53	0.22
Conductivity/ mS dm^{-1}	74–1591	324
Major components (%)		
SiO ₂	69.3–28.2	47.5
Al ₂ O ₃	13.8–5.4	8.8
Fe ₂ O ₃	37.3–2.5	12.5
CaO	28.5–0.6	11.0
MgO	8.0–1.4	3.3
K ₂ O	3.2–0.8	2.0
MnO	0.28–0.04	0.13
TiO ₂	0.80–0.24	0.49
P ₂ O ₅	0.28–0.05	0.13

Table 2 Definition of fractions and extraction conditions related to the SM&T-SES for chemical fractionation of soil samples

Nominal target phase	Reagent and conditions	Comments
Exchangeable + acid- and water-soluble	Shaking for 16 h with 0.11 mol l ⁻¹ acetic acid	Weakly-bounded metals retained on soil surface by relatively weak electrostatic interactions, which can be released by changes in ionic composition, modifications of adsorption or desorption of metals on sediment constituents or affected by production or consumption of protons. Often considered representative of available amounts.
Reducible	Shaking for 16 h with 0.5 mol l ⁻¹ hydroxylammonium chloride, pH = 1.5	Trace elements contained on iron and manganese (hydr)oxides are released, because of their thermodynamic instability under anoxic conditions and dissolution of metal-oxide phases under controlled Eh and pH conditions.
Oxidable	Digestion with hydrogen peroxide at room temperature, evaporation, redigestion and evaporation, then shaking for 16 h with 1.0 mol l ⁻¹ ammonium acetate	Trace elements bounded to various forms of organic matter as biotic detritus, organic coatings on inorganic particles or living organisms. The degradation of organic matter under oxidizing conditions is responsible for releasing trace elements.
Residual	Digestion with Aqua Regia (ISO 11466 protocol)	Trace elements in the lattice of primary and secondary minerals. In this case possible changes in environmental conditions would have no effect on the release of metals from this fraction on a time-scale of several years.

nebulizer fouling when using ICP-MS or ICP-OES. The resulting extracts were placed in polypropylene bottles and stored at 4 °C prior to analysis, except extracts from the second step, which were analysed immediately due to instability and degradation of the extracting reagent. All experiments were performed in triplicate, including the control samples for the vessel, reagent and procedural blanks. Relative standard deviations of the results were typically below 12%. Higher deviations were observed for some samples due to both very low concentrations of the measured metal and heterogeneity of soil samples.

Apparatus and reagents

Major components were determined using a Philips PW2400 X-ray spectrophotometer with Rh excitation tubes and a Philips radio-frequency inductive oven (model PERL'X2, Holland). HMs were determined in both the three steps of SES and *aqua regia* digests, using a ARL minitorch inductively coupled plasma optical emission spectrometer (ICP-OES) (model 3410, Valencia, CA, USA). For trace elements below ICP-OES detection limits, a ThermoElemental inductively coupled plasma mass spectrometer (ICP-MS) (model PQExcell, Windsford, UK) was employed. Quantification of HMs was with respect to reagent-matched standard solutions, obtained by serial dilution of commercial stock solutions (Merck Darmstadt, Germany and J. T. Baker, North Kingstown, RI, USA). Multi-element standard solutions were used for ICP-OES and ICP-MS. Analytical grade reagents, supplied by Panreac, Barcelona, Spain, J. T. Baker, Phillipsburg, NJ, USA, or Merck, Darmstadt, Germany, were used throughout. All glassware and plastic containers were previously soaked overnight

in 25% nitric acid and rinsed with double distilled water. Sample digestions for pseudototal determination were performed in perfluoroalcoxy (PFA) vessels, with a CEM Corporation microwave laboratory unit (CEM Mars X, Mathews, NC, USA). Conventional sequential extraction was performed using a SBS end-over-end mechanical shaker (model ABT-4, Barcelona, Spain). Extracts were separated from solid residues using a Pacisa centrifuge (model C-5, Barcelona, Spain).

Multivariate statistical analysis

Chemometric techniques for pattern recognition were applied to the analytical SES data obtained from the 21 samples analysed.⁴¹ The combined function of scores and loadings identifies both the groups of samples with similar behaviour and the existing correlations between the original variables. The corresponding data matrix includes the six metal concentrations in each of the four fractions plus the edaphological parameters of samples. Data was processed by applying Principal Component Analysis (PCA) as well as Hierarchical Cluster Analysis (HCA) in order to gain knowledge on the distribution of pollutants by detecting similarities and differences between the data. Factor analysis was performed by evaluation of principal components and computing the eigenvectors higher than 1 (Kaiser Criterion). Afterwards, the rotation of principal components was carried out by Varimax normalized algorithm which allows an easier interpretation of the principal component by both maximizing the variance of the extracted factors and reducing uncertainties that accompany initial unrotated factor loadings. Varimax Rotation of the matrix was applied after factor analysis, using those principal components that contribute more than 5% of the

Table 3 Determined, certified and indicative values (mg kg⁻¹) for CRM BCR 701 extractable trace elements in sediments following SM&T-SES

	F1 (Acid soluble fraction)		F2 (Reducible fraction)		F3 (Oxidable fraction)		(Pseudototal content)	
	Determined ^a	Certified	Determined	Certified	Determined	Certified	Determined	Indicative ^b
Cd	7.0 ± 1.1	7.3 ± 0.4	3.1 ± 0.2	3.8 ± 0.3	0.24 ± 0.04	0.27 ± 0.06	11.4 ± 0.8	11.7 ± 1.0
Cu	49 ± 3	49.3 ± 1.7	116 ± 4	124 ± 3	55 ± 7	55 ± 4	272 ± 5	275 ± 13
Ni	16.7 ± 0.5	15.4 ± 0.9	27.9 ± 0.7	26.6 ± 1.3	15.8 ± 0.8	15.3 ± 0.9	101 ± 2	103 ± 4
Pb	3.6 ± 0.4	3.2 ± 0.2	119 ± 3	126 ± 3	11.0 ± 1.5	9 ± 2	141 ± 3	143 ± 6
Zn	202 ± 7	205 ± 6	112 ± 2	114 ± 5	45 ± 2	46 ± 4	450 ± 8	454 ± 19

^a Results are expressed as the mean of four determinations ± standard deviation. ^b Indicative values obtained from BCR 701 certificate.

total variance of the data set. In addition, HCA was applied using Ward's method of agglomeration and squared Euclidean distance as the measurement of similarity. Correlation between parameters, PCA and HCA were applied using SPSS v10.0 and XIStat v5.2 statistical computer programs.

Results and discussion

Five metals, Cd, Cu, Ni, Pb and Zn and the metalloid As, were determined in the different soil samples extracts, both those obtained from the SES application and those resulting from digestion procedures. Corresponding concentration values related to dry matter weight are statistically summarized in Table 4 and the whole dataset is shown in Table ESI-1.† The data obtained correspond to the areas close to the ditches network of the mining site, so the pollution assessment will be limited to this area.

A basic consideration refers to the background level of metals in soils as a result of natural phenomena,⁴² such as the contribution of parent material, common anthropogenic activities, agriculture, traffic, *etc.* Then, pollution is confirmed when metal concentrations are higher than typical values for soils found in the literature and exceed the levels present in nearby areas. To this extent, the results of pseudototal content were compared with maximum acceptable concentrations in soils, reported for reclamation of contaminated sites following the Dutch intervention values⁴³ as well as the French legislation⁴⁴ values given in Table 5. On the other hand, it is known that high pollutant concentrations accompanied by high standard deviations suggest anthropogenic sources, while homogeneous distribution across the site and therefore lower standard deviations, indicate a major natural source or lithogenic character.⁴⁵

In the case of the Salsigne site, all samples exceed the Dutch intervention values for As, Cd and Cu (except sample 24), for Ni only sample 9, Pb (except samples 7, 8, 13, 19, 23, 24) and Zn (except samples 4–8, 13, 16, 19, 24), indicating that the pollution has anthropogenic sources. Although high levels of heavy metals have been reported in sedimentation areas of contaminated soils in the vicinity of metalworking factories and mining areas, Salsigne values are exceptionally high, so, the site can be considered as "critically polluted". In particular, while As is the major pollutant, Cu, Pb and Zn content also has to be considered to properly assess the pollution level at the site. In addition, when considering the data from the first step of the SES (mobile fraction), a considerable number of samples also surpass the mentioned Dutch levels.

Data transformation

Because of the high positive and negative skewness of some of the primary data, appropriate data transformation is needed for a suitable statistical treatment. Furthermore, possible outliers must also be identified because strongly skewed distributions and outliers can contribute to biased conclusions in statistical analyses. In our case, the obtained data are both

skewed and sharply distributed. Skewness is due to particularly high values of As and Zn in some of the samples. On the other hand, kurtosis is observed because of data clustering at low values of target variables for the majority of samples. Such behaviour reveals a lack of normal distribution of the data. For this reason, a logarithmic transformation was applied that resulted in a general smaller skewness and kurtosis of most variables (except Ni in F2 and F4, Pb in F2 and Zn in F3). This transformation is widely applied in order to normalise positively skewed data sets.

However, such a transformation of environmental data sets does not always follow lognormal distributions. In such cases, a different transformation is needed, and Box–Cox transformation is one of the most frequently used.^{46,47} This transformation is given by the equation listed below

$$y = \begin{cases} \frac{x^\lambda - 1}{\lambda} & \lambda \neq 0 \\ \ln(x) & \lambda = 0 \end{cases}$$

where y is the transformed value and x is the value to be transformed. For a given data set (x_1, x_2, \dots, x_n), the parameter λ is estimated by considering the transformed values (y_1, y_2, \dots, y_n) to follow a normal distribution. When $\lambda = 0$, the transformation becomes a logarithmic transformation. In our case, it was observed that Box–Cox transformation conferred normality on the data more effectively than did logarithmic transformation, except for conductivity and Pb(F1) and Ni(F3) concentrations. The Box–Cox transformed data sets of the rest of variables accomplished with the normal distribution test at the significance level of 0.05. Because almost all the Box–Cox transformed data sets follow the normal distribution, they were used for the statistical analysis as described below.

Treatment of pseudototal metal content data

From the available dataset, after the application of PCA treatment to the pseudototal metal concentration transformed data, a significant correlation (above 0.7 for a 0.05 level of significance) is observed between some variables, being most significant for Ni and Zn or Cu and Pb. The contribution to total variance of the first three PCs is 48%, 20% and 12%, respectively (80% in all). Cu, Ni, Pb and Zn concentrations mainly describe the first component, while the second component depends strongly on pH and the third component increases with organic matter content, O.M.%. The combined plot of scores and loadings of PC1 vs. PC2 shown in Fig. 2(a) observes that PC1 accounts for the pollution of the site and classifies samples with similar pollutant content in two different groups and two outlier samples (S9 and S15) at the opposite extremes of the site. Within the first group, samples S4, S6–8, S13, S21–24 are included. Their common characteristics are concerned with a low level of contamination and their location on the site at the beginning of ditches. Taking into account the pseudototal concentration, these samples could be considered as representative samples of the lithogenic background. The other group of samples containing S1–3, S5, S10–12, S16–19,

Table 4 Statistical summary of mean, median, and minimum and maximum element concentrations for the sequentially extracted fractions of Salsigne samples by means of SM&T-SES. (mg kg⁻¹)

	F1 (Acid soluble fraction)	F2 (Reducible fraction)	F3 (Oxidable fraction)	(Pseudototal content)
As	384 ^a , 26 (0.8–3840) ^b	2899, 1211 (40–13873)	344, 228 (96–837)	11333, 5820 (643–53104)
Cd	5.6, 1.9 (0.2–45)	6.6, 3.3 (0.01–48)	1.7, 0.9 (0.01–12)	38, 29 (2–145)
Cu	616, 87 (0.01–3706)	449, 152 (0.01–2715)	509, 230 (23–2044)	2345, 1134 (80–9790)
Ni	12, 9.6 (1.1–47)	16, 8.6 (0.01–68)	25, 25 (10–46)	86, 55 (21–522)
Pb	20, 2.6 (0.01–338)	246, 118 (0.01–1362)	49, 26 (2.9–255)	730, 564 (69–3566)
Zn	414, 103 (0.01–3779)	344, 195 (6.6–2888)	230, 111 (0.01–2469)	1678, 769 (69–15639)

^a First value represents the arithmetic average of 21 samples, second value represent the median of 21 values. ^b Minimum and maximum values, respectively.

Table 5 Typical concentration ranges and most common values present in soils,⁴² average abundance in earth's crust, target and intervention values in Dutch legislation,⁴³ values for sensitive and non-sensitive use in French legislation.⁴⁴ (Values in mg kg⁻¹ unless otherwise stated)

Range	Common values ^a	Earth's crust	Dutch legislation		French legislation	
			Target values	Intervention values	Sensitive use	Non-sensitive use
As			29	55	37	120
Cd	0.01–2.0	0.2–1	0.15	0.8	12	60
Cu	2–250	20–30	70	36	190	—
Ni	2–750	50	80	35	210	140
Pb	2–300	10–30 (rural) 30–100 (urban)	16	85	530	400
Zn	1–900	50	220	140	720	9000

^a Values for agricultural soils.

are those samples located at the intermedius and final segments of the ditches network, the high Cd, Cu, Ni, Pb and Zn content being the main variables contributing to PC1 (see Fig. 2(a)). These samples are related to the continuous input of HMs to the catchment areas associated with these sampling points. In this area, close to the warehouse and storages neighbourhood is where the continuous erosion and deposition of waste have led to the accumulation of such a huge amount of heavy metals. Samples S9 and S15 could be catalogued as outliers in Fig. 2(b) due to a high content of As (improper storage of AsO₃ waste), and high amounts of Zn (because of an enriched Zn-slag treatment area), respectively.

Statistical data processing (SM&T-SES fraction contents)

For the SM&T-SES first fraction, PCA is able to extract three PCs that contribute to 79% of the total variance; PC1 (42%) is dominated by HMs contribution, while PC2 (21%) will explain pH and conductivity behaviour and PC3 (13%) is loaded with O.M.%. From the selected plot of Fig. 3(a), where PC1 vs. PC2

are represented, the available content of samples increases with PC1 being S1, 2, 9, 10; those samples that represent the most hazardous area at the end of the ditches network. Less polluted samples, in terms of HMs release under acidic conditions, S13, 15, 23, 24, are inversely correlated to this PC but in a more widely spread distribution. The rest of the samples with an intermediate available HMs content lie between previously indicated groups. Results from the dendrogram in Fig. 3(b) confirm the observed three groups differentiated by the available content when a 20% dissimilarity is selected.

For the second fraction of SM&T-SES, again three PCs contribute to a total variance of 71%. In this case, the loading of the extracted PCs is different from that obtained when considering the first fraction content. PC1 (47%) is mainly related to all HMs except Zn which loads PC2 together with pH (12%) and finally O.M.% in PC3 (11%). Accordingly, by plotting PC1 vs. PC2, the discrimination depending on the amount of HMs available under reducing environmental conditions and their distribution on the site can be interpreted similarly to the distribution of pseudototal and first fraction

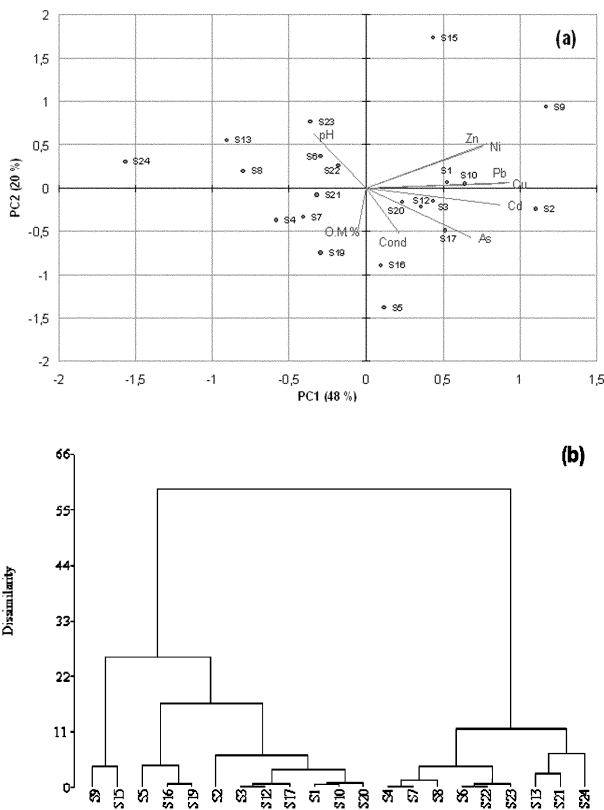


Fig. 2 (a) Combined plot of scores and loadings for the released pseudototal amount of metals in the digestion of soils after Varimax rotation. (b) Dendrogram obtained by cluster analysis of pseudototal metal concentrations.

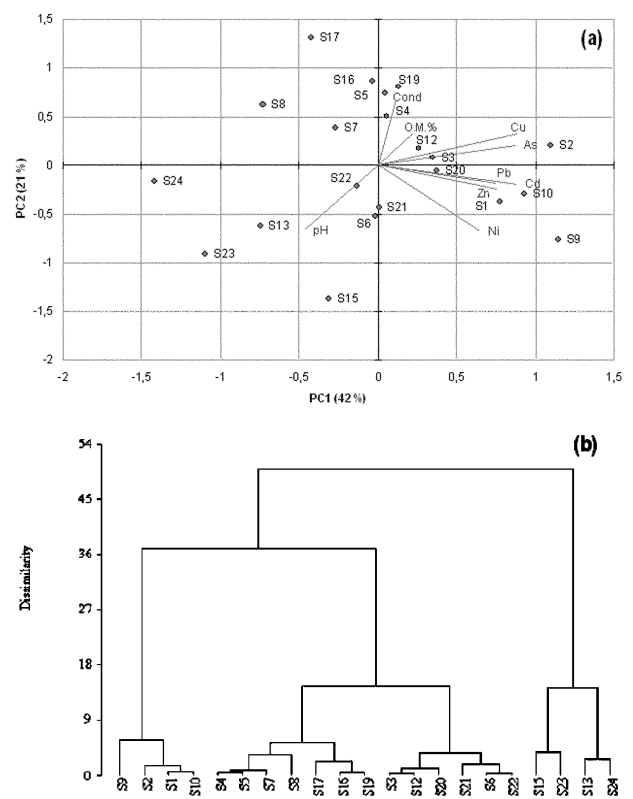


Fig. 3 (a) Combined plot of scores and loadings for the extracted amounts of metals in the first fraction of SM&T-SES after Varimax rotation. (b) Dendrogram obtained by cluster analysis of the extracted metals in the first fraction of SM&T-SES.

content. However, samples (e.g. S1) will be classified in different groups because of the selected fraction. Samples with a high available amount under reducing conditions show a positive score (S2, 3, 9, 10 and 17). Within the low level polluted samples, widely distributed along PC1 with negative scores, and considering the obtained dendrogram in Fig. 4(b), two subgroups (S13, 15 and S7, 8, 23, 24) can be observed because of the high differences in available Zn. Specifically, S15 owes its high Zn content to enriched Zn-slag deposits. In this respect, S13 receives the influence of the S15 area, while the S7, S8, S23 and S24 area observes a minor influence of mentioned deposits due to natural diffusion barriers. Classification of the rest of the samples, having intermediate concentrations available, is less clear since target parameters of pollution have no specific differentiation (i.e. variables contributing to PC1 are not relevant enough to show a similar discrimination to that observed in high and low level polluted samples).

In the third fraction of SM&T-SES, discrimination between samples is more difficult that in previous fractions, which may be linked to the low-extracted amounts of HMs, now representing the available amount of HMs under oxidizing conditions (bound to O.M.). Four components are extracted contributing to a total variance of 78%, with PC1 (32%) having high loadings of all HMs except As while O.M.% dominates PC2 (21%), pH mainly contributes to PC3 (13%) and As loads PC4 (11%). The correlations among samples, observing the plot of PC1 vs. PC2 in Fig. 5(a) and dendrogram in Fig. 5(b), have to be understood in terms of pH, Cu and Zn content, with samples S1, 2, 9, 10, 12, 20, 21 being those with a high amount of available HMs under oxidizing conditions. The rest of the samples present lower available amounts, with S4, S8 and S19 being less polluted. Intermediate polluted samples are grouped into two clusters at each side of highly polluted samples and are differentiated by their common pH. Despite a few differences in some samples, a similar spatial distribution is observed as those previously extracted in the other fractions

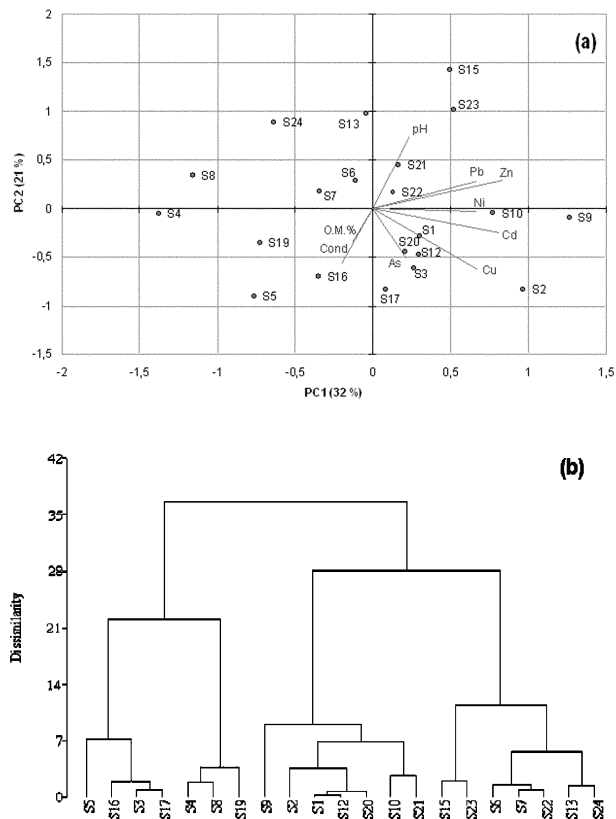


Fig. 5 (a) Combined plot of scores and loadings for the extracted amounts of metals in the third fraction of SM&T-SES after Varimax rotation. (b) Dendrogram obtained by cluster analysis of the extracted metals in the third fraction of SM&T-SES.

when considering the available amount of HMs under oxidizing conditions.

Interpretation of sequential extraction results

From the statistical analysis and considering the anthropogenically-induced pollution, there are three main groups of samples that can be clearly differentiated by metal mobility, which belong to different segments of the ditch network. In general terms an increase in the available content is observed when the pseudototal content increases.⁴⁸ A representative average value of the fractionation pattern for each element in each group is shown in Fig. 6 which illustrates the specific mentioned differences. Also, significant correlations between HMs fraction contents and major matrix components were determined using the non-parametric Spearman correlation coefficient (r_s), which is based on ranks, is insensitive to outliers and does not requires data normality.⁴⁹

A common observed trend in the highly polluted samples (final segment of ditches network) that we classify as group I, Fig. 6(a), includes a high availability of Cd and Zn, indicated by the data of the first fraction content. The available Cu amount also has to be remarked upon. Although this element is frequently associated with the oxidable fraction,⁵⁰ the observed Cu in the first fraction may result from the overloading of possible organic binding sites and the characteristics of anthropogenic surface pollution which displays less adsorption and is preferably linked by weak interactions of contaminants with phase components. It is also interesting to note that almost 70% of the pseudototal Pb amount could be released under reducing conditions, F2, representing a high exposure risk. It is in these samples that the preferred association of Pb with iron and manganese oxides is well illustrated.⁵¹ However, the reducible Pb contents are significantly anticorrelated ($\alpha = 0.05$) with the MnO content ($r_s = -0.962$). This value can be

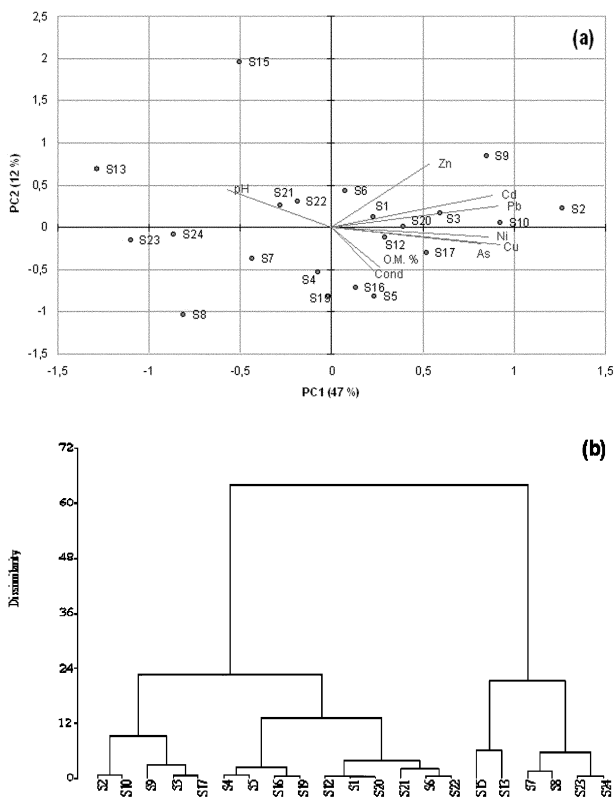


Fig. 4 (a) Combined plot of scores and loadings for the extracted amounts of metals in the second fraction of SM&T-SES after Varimax rotation. (b) Dendrogram obtained by cluster analysis of the extracted metals in the second fraction of SM&T-SES.

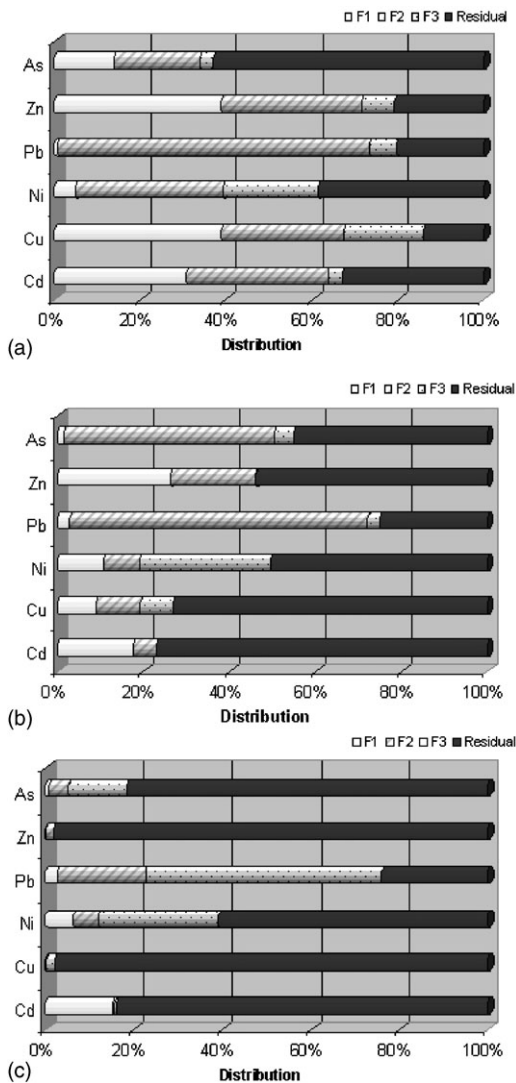


Fig. 6 Representative fractionation patterns of HMs resulting from the statistical analysis of the whole data set. (a) Group I, (b) Group II and (c) Group III.

understood as an oversaturation of this component in the reducible fraction. The relatively low proportion of As in the first fraction (10%) may lead to a misinterpretation of the pollution impact, since the high As content actually means that the first fraction exceeds by a factor of forty the maximum level allowed for intervention purposes. Concerning As distribution, the major residual fraction can be as a result of both the lithogenic characteristics of the site and the ancient mining activity that provided a continuous input of arsenic to soils. For Ni distribution, most characteristic is the 40% release under reducing conditions that follows the trend of Pb. The samples classified within this group represent the areas surrounding the final segment of the ditches network; the most polluted area, due to both surfaces with the highest amount of disposed waste related to the warehouse area and the accumulation process from the rest of the ditches network.

In samples from the middle stretch of ditches, group II, Fig. 6(b), similar trends and associations as those previously commented on in highly polluted samples are depicted. However, a net reduction is observed in the degree of availability as well as an increase of HMs content in the residual fraction, indicating a general reduction in HMs mobility that can be due to a higher lithogenic nature of these samples. Accordingly, a remarkable reduction of Cu mobility and availability, against group I, is observed. Thus, the sum of the first three fractions does not exceed 25% of the pseudototal amount. The signifi-

cant anticorrelation ($\alpha = 0.05$) of the Cu oxidable content with SiO_2 and Al_2O_3 ($r_s = -0.744$ and -0.678 , respectively) reveals the affinity of Cu to the residual fraction. On the other hand, Cd and Zn present the highest mobility by considering their first fraction content, that together with the absence of these metals in the oxidable fraction indicate the possible anthropogenic origin of these metals. Pb shows almost the same distribution as in highly polluted samples except a slight increase in the residual fraction. Therefore a considerable Pb hazard is still observed under reducing conditions. The residual Pb increase correlates significantly ($\alpha = 0.05$) with SiO_2 , Al_2O_3 and Fe_2O_3 content ($r_s = -0.638$, -0.689 , 0.870 , respectively), denoting the preferred association of Pb with the crystalline Fe_2O_3 component. Conversely, a clear modification of the fractionation pattern is observed for As distribution since the reducible fraction increases in this group. This fact is corroborated by a significant correlation ($\alpha = 0.05$) of As reducible content with Fe_2O_3 content ($r_s = 0.863$). It is important to note that a similar misinterpretation as in heavily polluted samples can be observed, in this case, for the second fraction content (almost 40% of the pseudototal amount is available). In this group, the Ni distribution along the oxidable fraction has increased, probably due to the Ni affinity for the less leacheable fractions (organic matter and residual matrix).

In group III, (samples of lowest pollution) Fig. 6(c), there is a net reduction of the mobility and a general major residual distribution of some elements such as Zn and Cu, in contrast with previous groups. These aspects indicate a main lithogenic origin of these elements, such as Zn occlusion into stable structures such as crystalline Fe_2O_3 , rather than anthropogenic pollution. It is interesting to note that for Zn the released contents in every fraction are significantly correlated ($\alpha = 0.05$) to Fe_2O_3 content ($r_s = 0.952$ F1, 0.973 F2, 0.986 F3, 0.940 Residual). However, Cd and Ni distributions are quite similar to those present in the highly polluted samples from group II, although the pseudototal content of these samples is lower than group II samples, but still above intervention values. For Pb, the main association is observed with the oxidable fraction, which can be understood to be more of lithogenic rather than anthropogenic origin. This is corroborated by a significant correlation ($\alpha = 0.05$) in the reducible fraction between Pb content and Fe_2O_3 and MnO ($r_s = 0.855$ for Fe_2O_3 and 0.864 for MnO). The residual phase also presents a significant correlation of Pb content with Fe_2O_3 ($r_s = 0.966$) suggesting the occlusion of this element within crystalline structures resistant to leaching conditions. Arsenic also presents a major residual content, and the corresponding concentrations are lower than in groups I and II. These observations are related to samples from the initial segment of the ditches, where catchment areas contributing to ditches are less polluted than in the final area. Also, the steeped topography of the area avoids the accumulation process, thus reducing the pollution observed in these samples.

Conclusions

Application of suitable statistical analysis to SES raw data of HMs concentration in mining polluted soils requires a previous Box-Cox transformation of strongly skewed data to effectively normalise such data and diminish the negative effect of outliers. Such analysis reveals similarities or differences among samples as well as correlations or anticorrelations between variables, illustrating the extension and distribution trends of HMs in the studied area. These polluted soils show a high level of As, Cu, Cd, Pb and Cu contamination, anthropogenically enhanced by mining activity. Along the studied areas surrounding the ditches network, it is possible to distinguish three groups of samples having a general increase of pollution that enhances the mobility and availability of the studied HMs. However, some areas at the middle of the ditches network can

be identified as localised hot spots with an abnormal amount of a single element related to former waste and slag disposal areas.

From partitioning data, it is possible to conclude that there are significant differences in the distribution of the studied HMs, with Cd and Zn being the most mobile HMs. Consequently, an easier exchange of these elements between the soil and the water column is expected, independently of sampling points. The main hazard of other HMs such as As and Pb is related to their availability under reducing conditions.

In spite of the limitations of sequential extraction procedures, the value of the information obtained by using the statistical analysis of data presented here can be appreciated in the risk assessment of such polluted sites as well as in addressing specific solutions for their appropriate remediation.

Acknowledgements

The authors thank IRH (France) for their help in collection, preparation and supplying samples from the Salsigne contaminated site. Financial support has been provided by DIMDES-MOTOM European project (EVK1-CT-1999-00002). Universitat Autònoma of Barcelona is also acknowledged for providing a scholarship grant to G. Pérez.

References

- 1 A. V. Filgueiras, I. Lavilla and C. Bendicho, *J. Environ. Monit.*, 2002, **4**, 823.
- 2 M. Kersten and U. Förstner, in *Trace Element Speciation: Analytical Methods and Problems*, ed. G. E. Battley, CRC Press, Boca Raton, FL, 1989, pp. 245–317.
- 3 D. M. Templeton, F. Ariese, R. Cornelis, L. G. Danielsson, H. Mutuau, H. P. Van Leeuwen and R. Lobinski, *Pure Appl. Chem.*, 2000, **72**(8), 1453.
- 4 A. K. Das, R. Chakraborty, M. L. Cervera and M. De La Guardia, *Talanta*, 1995, **42**, 1007.
- 5 G. Rauret, *Talanta*, 1998, **46**, 449.
- 6 F. M. G. Tack and N. G. Verloo, *Int. J. Environ. Anal. Chem.*, 1995, **59**, 225.
- 7 A. Tessier, P. G. C. Campbell and M. Bisson, *Anal. Chem.*, 1979, **51**(7), 844.
- 8 G. Rauret, R. Rubio and J. F. López-Sánchez, *Int. J. Environ. Anal. Chem.*, 1989, **36**, 69.
- 9 J. L. Gómez-Ariza, I. Giráldez, D. Sánchez-Rodas and E. Morales, *Sci. Total Environ.*, 2000, **246**, 271.
- 10 A. Barona, I. Aranguiz and A. Elías, *Chemosphere*, 1999, **39**(11), 1911.
- 11 C. M. Davidson, A. L. Duncan, D. Littlejohn, A. M. Ure and A. L. Garden, *Anal. Chim. Acta*, 1998, **363**, 45.
- 12 L. Fanfani, P. Zuddas and A. Chessa, *J. Geochem. Explor.*, 1997, **58**, 241.
- 13 E. C. Fonseca and E. F. Da Silva, *J. Geochem. Explor.*, 1998, **61**, 203.
- 14 C. Gommy, E. Perdrix, J. C. Galloo and R. Guillermo, *Int. J. Environ. Anal. Chem.*, 1998, **72**(1), 27.
- 15 S. O. Kim and K. W. Kim, *J. Hazard. Mater.*, 2001, **B85**, 195.
- 16 I. M. C. Lo and X. Y. Yang, *Waste Manage.*, 1998, **18**, 1.
- 17 I. Maiz, I. Arambarri, R. Garcia and E. Millan, *Environ. Pollut.*, 2000, **110**, 3.
- 18 J. E. Maskall and I. Thornton, *Water, Air Soil Pollut.*, 1998, **108**, 391.
- 19 J. Pichtel, K. Kuroiwa and H. T. Sawyerr, *Environ. Pollut.*, 2000, **110**, 171.
- 20 E. Galán, J. L. Gómez-Ariza, I. González, J. C. Fernández-Caliani, E. Morales and I. Giráldez, *Appl. Geochem.*, 2003, **18**(3), 409.
- 21 J. L. Gómez-Ariza, I. Giráldez, D. Sánchez-Rodas and E. Morales, *Int. J. Environ. Anal. Chem.*, 1999, **75**(1–2), 3.
- 22 A. E. González, M. T. Rodríguez, J. C. J. Sánchez, A. J. F. Espinosa and F. R. Barragán, *Water, Air Soil Pollut.*, 2000, **121**, 11.
- 23 L. Leleyter and J. L. Probst, *Int. J. Environ. Anal. Chem.*, 1999, **73**(2), 109.
- 24 J. Morillo, J. Usero and I. Gracia, *Int. J. Environ. Anal. Chem.*, 2002, **82**(4), 245.
- 25 R. Van Ryssen, M. Leermakers and W. Baeyens, *Environ. Sci. Policy*, 1999, **2**, 75.
- 26 E. A. Álvarez, M. C. Mochón, J. C. J. Sánchez and M. T. Rodríguez, *Chemosphere*, 2002, **47**(7), 765.
- 27 I. Lavilla, B. Pérez-Cid and C. Bendicho, *Anal. Chim. Acta*, 1999, **381**, 297.
- 28 J. Scanzar, R. Milacic, M. Strazar and O. Burica, *Sci. Total Environ.*, 2000, **250**, 9.
- 29 I. Walter and G. Cuevas, *Sci. Total Environ.*, 1999, **226**, 113.
- 30 A. A. Zorpas, T. Constantinides, A. G. Vlyssides, I. Haralambous and M. Loizidou, *Bioresour. Technol.*, 2000, **72**, 113.
- 31 Ph. Quevauviller, G. Rauret, H. Muntau, A. M. Ure, R. Rubio, J. F. López-Sánchez, H. D. Fiedler and B. Gierpink, *Fresenius' J. Anal. Chem.*, 1994, **349**, 808.
- 32 Ph. Quevauviller, G. Rauret, J. F. López-Sánchez, R. Rubio, A. Ure and H. Muntau, *Sci. Total Environ.*, 1997, **205**, 223.
- 33 A. M. Ure, Ph. Quevauviller, H. Mutuau and B. Griepink, *Int. J. Environ. Anal. Chem.*, 1993, **51**, 135.
- 34 C. Kheboian and C. F. Bauer, *Anal. Chem.*, 1987, **59**, 1417.
- 35 E. Tipping, N. B. Hetherington, J. Hilton, D. W. Thompson, E. Bowles and J. H. Taylor, *Anal. Chem.*, 1985, **57**, 1944.
- 36 S. Xiao-Quan and C. Bin, *Anal. Chem.*, 1993, **65**, 802.
- 37 C. Whalley and A. Grant, *Anal. Chim. Acta*, 1994, **291**, 287.
- 38 G. Bird, P. A. Brewer, M. G. Macklin, D. Balteanu, B. Driga, M. Serban and S. Zaharia, *Appl. Geochem.*, 2003, **18**, 1583.
- 39 Departament de Medi Ambient, Junta de Residus, Generalitat de Catalunya, *Pautes d'anàlisi*, Servei de Publicacions, Barcelona, Spain, 1998.
- 40 A. Sahuquillo, J. F. López-Sánchez, R. Rubio, G. Rauret, R. P. Thomas, C. M. Davidson and A. M. Ure, *Anal. Chim. Acta*, 1999, **382**, 317.
- 41 J. W. Einax, H. W. Zwanziger and S. Geiß, *Chemometrics in Environmental Analysis*, Wiley-VCH Verlag, Berlin, 1997, ch. 5.
- 42 H. J. M. Bowen, *Environmental Chemistry of the Elements*, Academic Press, New York, 1979.
- 43 D. C. Adriano, *Trace Elements in the Terrestrial Environment. Biogeochemistry, Bioavailability and Risk of Metals*, Springer Verlag, New York, 2001, ch. 6.
- 44 D. Darmendrail, *The French approach to contaminated-land management*, BRGM/RP-51098-FR, Bureau de Recherches Géologiques et Minières, Orléans, France, 2001.
- 45 D. S. Manta, M. Angelone, A. Bellanca, R. Neri and M. Sprovieri, *Sci. Total Environ.*, 2002, **300**(1–3), 229.
- 46 C. S. Zhang and S. Zhang, *GeoJournal*, 1996, **40**(1–2), 209.
- 47 C. S. Zhang, O. Selinus and J. Schedin, *Sci. Total Environ.*, 1998, **212**, 217.
- 48 T. U. Aualiita and W. F. Pickering, *Talanta*, 1988, **35**(7), 559.
- 49 R. A. Sutherland, *Environ. Forensics*, 2001(2), 265.
- 50 Y. Yin, C. A. Impellitteri, S. J. You and H. E. Allen, *Sci. Total Environ.*, 2002, **287**, 107.
- 51 W. F. Pickering, *Ore Geol. Rev.*, 1986, **1**, 83.

Decontaminating abandoned mines



Spanish chemists are helping to clean up disused industrial sites.

Before abandoned contaminated industrial sites can be recovered, the distribution and availability of pollutants have to be known in detail.

Motivated by this, Manuel Valiente and Gustavo Pérez from

A new approach improves analysis of heavy metal distribution

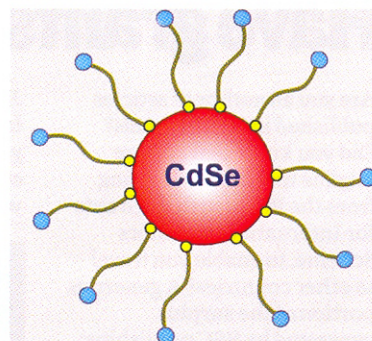
Reference
G Pérez and M Valiente, *J. Environ. Monit.*, 2005, **7**, 29

Barcelona analysed an abandoned 40 hectare open-cast mine at Salsigne, France, for various heavy metals.

To do this, the researchers used a sequential extraction scheme (SES). In this process a sequential series of selective extractant reagents, each a more powerful extractant than the last, is employed to selectively dissolve or solubilise the different solid phases or mineralogical fractions of heavy metals. In a new approach, Valiente combined the SES results with chemometric data processing to better determine the pollution trends and distribution of heavy metals in the studied area.

This combined approach bodes well for assessing other contaminated industrial sites. As Valiente comments: 'The value of the information obtained can be appreciated in the risk assessment of such polluted sites, as well as in addressing specific solutions for their appropriate remediation.' *Philip Earis*

Nanosensor for toxic anions



In a useful application of nanotechnology Spanish researchers have developed a sensitive toxic-cyanide sensor.

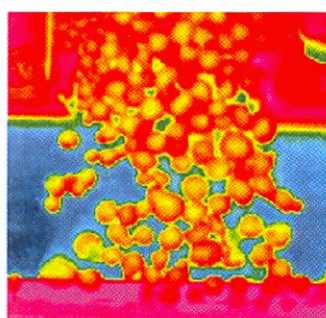
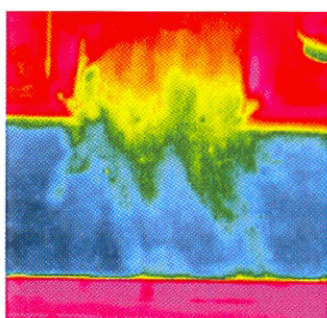
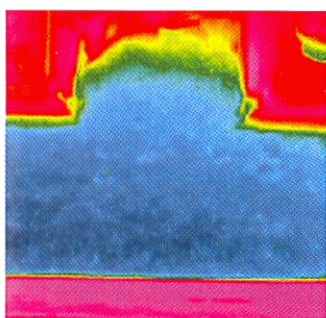
Nanometre-sized low-dimensional semiconductors known as quantum dots (QDs), look promising for numerous applications. However, to date the exploitation of QDs has mainly concentrated on optical imaging in biology and developments in optoelectronics.

With their extensive experience in luminescence sensing, Alfredo Sanz-Medel and his colleagues at the University of Oviedo reasoned that QDs could also be used in chemical sensing. They first modified the surface of cadmium selenide QDs to make them water soluble and then examined their properties in aqueous solution. Not only is the luminescence emission of their modified QDs very sensitive to the presence of even very low concentrations of cyanide ions in aqueous solution but it is also selective for the cyanide ion over other common anions.

Sanz-Medel has big plans for the future. 'Efforts should be directed to the field of surface modification of luminescent QDs (aiming at synthesising new sensing reagents with high specificity for a variety of chemical species) and in their immobilisation onto or into appropriate solid surfaces (avoiding their aggregation) in order to produce robust and reliable optical nanoprobes.' *Caroline Evans*

Reference
W J Jin *et al.*, *Chem. Commun.*, 2005 (DOI: 10.1039/b414858d)

Injecting powdered drugs



European researchers have developed two methods for separating and transporting tiny amounts of dry powders in microfluidic chips.

Producing new drugs is slow and increasingly needs to be speeded up to match the rate of drug development. This is particularly true of powder handling processes, which often only have a tiny amount of the synthesised drug available. Miniaturisation of powder handling is therefore desirable.

Now, Andreas Manz from ISAS, Germany, together with colleagues

Fluidised bed injection could be used in a chip-based system

Reference
T Vilckner, A Shivji and A Manz, *Lab Chip*, 2005 (DOI: 10.1039/b412566p)

at Imperial College London and Pfizer, UK, has been working on two techniques to manipulate powders. These techniques, termed fluidised bed injection and pulsed injection, could be integrated in a chip-based system for mixing dry powders on a small scale.

The team suggests the system could be used as an automated alternative to time-consuming manual weighing. Future work will look at approaches that can handle both dry and cohesive powders, because most drug excipients are cohesive. *Rowena Milan*

ANEXO 4

Assessment of readsorption during the chemical extraction of metals from soil and sediment CRMs.

A comparison of single extractions, ultrasonic and conventional sequential extractions

G. Pérez, M. Valiente, Cd. Bendicho. Submitted to Journal of Environmental Monitoring.

Assessment of readsorption during the chemical extraction of metals from soil and sediment CRMs. A comparison of single extractions, ultrasonic and conventional sequential extractions.

G. Pérez^a, M. Valiente^a, C. Bendicho*

^aCentre Grup GTS. Unitat de Química Analítica. Departament de Química. Universitat Autònoma de Barcelona. Facultat de Ciències. Edifici CN. 08193. Bellaterra, Barcelona, Spain.

*Universidad de Vigo. Departamento de Química Analítica y Alimentaria (Área de Química Analítica). Facultad de Ciencias (Química), As Lagoas-Marcosende s/n 36200. Vigo. Spain. Tel.: +34-986-812281. fax: +34-986-812556. e-mail: bendicho@uvigo.es

**This submission was created using the RSC Article Template (DO NOT DELETE THIS TEXT)
(LINE INCLUDED FOR SPACING ONLY - DO NOT DELETE THIS TEXT)**

Accelerated methods for partitioning of Cd, Cr, Cu, Ni, Pb and Zn, such as the use of single and ultrasonic extractions are assessed in terms of readsorption and compared with the three-stage sequential extraction scheme (SES) of the Standards Measurements and Testing Programme (SM&T). The standard addition approach was employed for characterising the readsorption artefact by applying the above fractionation methods over different certified reference materials (CRMs), BCR 701, BCR 601 (lake sediments), and BCR 141R soil. Ultrasonic extractions provided higher readsorption, mainly for BCR 141R and 601 as compared to conventional SES, the role of ultrasound in the activation of adsorptive sites being significant. The single extraction approach seemed to be inadequate with samples containing large amounts of carbonates such as BCR 141 R but worked well with both lake sediments. The readsorption phenomena are mainly occurring in the most labile fraction (i.e. acid soluble) and has been observed to be matrix dependent. The extent of such phenomenon is also dependent on the extraction methodology, i.e. conventional vs accelerated.

Introduction

Since Tessier's contribution¹ and the Community Bureau of Reference (BCR) harmonization,² sequential extraction schemes (SESS) have been widely applied and, thus, received an increasing attention during last years to estimate metal mobility and availability in the environment.³ Several methods for speeding up metal fractionation in order to overcome the time-consuming drawback of SESSs, such as application of single extractions or microwave and ultrasonic treatments, have been developed. Single extractions⁴ as a simple modification of SESSs, i.e. just performing simultaneously the extractions over different aliquots of the same sample, allow diminishing the whole treatment up to a day. The fraction contents, except the first one, are evaluated by subtracting the results obtained in two consecutive stages. On the other hand, ultrasonic versions of SESSs have demonstrated their potential for drastic acceleration of conventional SESSs, providing similar extractability for several metals in a variety of environmental samples.⁵⁻⁹ Microwave treatments may be less suitable for shortening the operation time in SESSs since the heating could cause significant changes on metal extraction and fractionation, being the labile fractions the most affected.¹⁰⁻¹³

The readsorption artefact has been identified as one of the most significant problems affecting the results obtained by sequential extractions.¹⁴ As a result of readsorption, the concentration of trace metals associated with the dissolving phase is underestimated whereas the concentration of trace metals associated with the receiving phase is overestimated. Three different approaches have been employed to assess the extent of readsorption, i.e. use of model synthetic phases, natural sediments spiked with model synthetic phases and the standard addition method. Kheboian and Bauer,¹⁵ using model synthetic phases, observed a significant readsorption of Cu, Pb and Zn when the Tessier scheme was applied. Ajayi and Vanloon¹⁶ employed the natural sediments spiked with model synthetic phases with the aim of supplying fresh unoccupied sites for

retention of any metals released during extraction. The main readsorption was attributed to Cr, Pb and Zn over iron and manganese oxides and organic matter. However, using a slightly modified second approach over the BCR-SES, Whalley *et al.*,¹⁷ observed that certain model phases e.g. humic acids and ferrihydrite generally released trace metals earlier than expected. Thus, both approaches, employing artificial model phases, differ markedly from natural sediments, thus biasing the system towards trace metal redistribution.

The observed drawbacks in the readsorption assessment by the commented approaches are overcome by the standard addition method. This would be an appropriate approach provided that the spiked metal concentrations were below 100% of the natural existing concentrations in the studied samples; otherwise the readsorption problem would be confused with a probably biasing of the system towards metal redistribution.¹⁸ Anyway, the standard addition should not exceed the native concentration in the sample so that the existing equilibrium is not significantly perturbed by the alteration of the extraction conditions.

To our knowledge, accelerated fractionation methods applied to obtain fast information about extractable metal contents have not been characterised in respect to readsorption in the SM&T-SES (Standard Measurements and Testing Program, formerly BCR-SES). Therefore, the aim of this work is to study the extent of the readsorption artefact when using, on one hand, ultrasonic extractions, and on the other hand, single extraction methodology to a conclusive comparison with the conventional SM&T-SES.

Experimental

Apparatus and Reagents

Cd, Cr, Cu, Ni, Pb and Zn were determined in both, extracts and *aqua regia* digests, using a Perkin Elmer inductively coupled plasma optical emission spectrometer (ICP-OES-axial view)

(model Optima 4300 DV, Norwalk, CT, USA). Matrix-matched standards with extractants were used for calibration. Calibration standards and reagent blanks were frequently reanalysed as samples for quality control purposes. Analytical grade reagents (Panreac and Merck) were used throughout. All extractant, standards, and rinse solutions were made from ultrapure water with a resistivity greater than 18 M Ω -cm, using a Milli-Q water purification system (Millipore, Molsheim, France). All glassware and plastic containers were previously soaked overnight in 25% nitric acid and rinsed. Sample digestions for *pseudototal* determination were performed in perfluoroalcoxy (PFA) vessels, with a CEM Corporation microwave laboratory unit (CEM Mars X, Mathews, NC, USA). Ultrasonic agitation was performed using a 100 W, 20 KHz probe sonicator (Sonics and Materials; model VC 100), equipped with titanium probes. Extracts were separated from solid residues using an Alresa centrifuge (model C-5, Barcelona, Spain). A Crison pH-meter (model 2001 micropH) was used for pH adjustments of the extracts.

Certified reference materials

Three certified reference materials (CRMs) were employed in this study for assessing readsorption, a description of their main characteristics being shown in Table 1. Among the considered CRMs, BCR 701 and 601 are both lake sediments, while BCR 141R is a heavy metal contaminated soil. BCR 701, 601 and 141R were obtained from the SM&T of the European Commission. BCRs 701 and 601 are provided with certified/indicative fraction-specific metal concentrations according to the modification of the BCR-SES that lead to the SM&T-SES.¹⁹ No sequential extraction data is available for BCR 141R, which provides only *aqua regia* soluble contents. Major compositions and total extractable metal contents of the CRMs studied are shown in Table 1.

Analytical procedures

Extraction conditions corresponding to each stage of the employed SM&T-SES are shown in Table 2. An ultrasonic version of this SES was applied following previously optimised conditions for treatments with an ultrasonic probe.⁶ To properly compare individual results of each fraction, ultrasound extractions were always applied over the remaining residues after removal of the previous fractions using the conventional SES. The single extraction approach followed the same operational conditions than the conventional procedure shown on the left of the table, but over fresh samples in every step. Accelerated and conventional extractions were performed by triplicate, including samples, vessel, reagent and procedural blanks, which were run simultaneously. As a quality control, a mass balance was established by comparing the *pseudototal* metal content (i.e. applying a microwave digestion with HCl+HNO₃) with the sum of the extracted metal percentages in the four steps. After each step of SES, the suspension was centrifuged and the supernatant from the solid phase separated. Extracts were filtered through 0.22-micron filter Millex-GS (Millipore, Ireland) in order to avoid the clogging of the nebulizer when using ICP-OES. The resulting extracts were stored in polypropylene bottles refrigerated at 4°C prior to analysis, with the exception of the extracts corresponding to the second fraction, which were analysed immediately due to the instability and degradation of the extractant reagent.

In order to compare the relative extractability of the fractionation approaches tried, the term ‘recovery’ was employed as in earlier studies,^{6,13} which is defined as follows:

Recovery (%) = [Metal released by ultrasonic or single extractions] / [Metal released by the conventional three-stage SES] × 100

Standard addition experiments

Experiments were addressed to estimate the extent of the readsorption phenomena of each metal (Cd, Cr, Cu, Ni, Pb and Zn) in every fraction of the SM&T-SES. Firstly, the conventional procedure was carried out in order to determine the appropriate metal amounts to be spiked in a particular fraction. Then, a new SES was performed on a separate sample portion after appropriate addition of small volumes (50-300 μ l) of acidified metal stock solutions. Thus, for F1 readsorption estimation, the spike was added to a fresh sample portion. For F2 and F3, the corresponding spikes were added to the remaining portions generated after F1 and F2 of the conventional SES, respectively. The spikes contained no more than 100% of the “native” extracted amount by the conventional SES, in order to maintain the normal extraction conditions.

In order to check for possible bias that could affect the assessment of readsorption, other different source of metal losses than that corresponding to the readsorption artefact were investigated. The blank experiments using the same volume of spiked extractant reagent showed that no losses by adsorption onto the wall of the treatment vessels were present during the sequential extraction experiments. On the other hand, non-significant metal amounts were detected in the rinsing water. Readsorption values (%) were obtained considering the difference between the measured concentrations (μ g/mL) of the metal in the extracts corresponding to treatments with non-spiked [M]_A and spiked [M]_C extractant. This difference was compared with [M]_B, which is the concentration (μ g/mL) of the element added to the extractant before the treatment. The readsorption (%) is calculated as follows:

$$\text{Readsorption (\%)} = \{1 - ([M]_C - [M]_A) / [M]_B\} \times 100$$

Results and discussion

Fractionation patterns

Fractionation patterns of Cd, Cr, Cu, Ni, Pb and Zn are depicted in Figure 1. Ultrasonic extractions, single extractions and conventional SES are compared. Firstly, CRM BCR 601 and CRM BCR 701 were employed for validation of SM&T-SES. In all cases, a good agreement between certified/indicative and found extractable contents is observed (Table 3).

It would be expected that in terms of recovery, single extractions did not significantly change the fractionation patterns of the considered metals and gave a similar performance, since the first fraction is common to the conventional procedure and operational conditions (e.g. extractant concentration, agitation time, temperature, etc) remain unchanged. However, while no significant differences between single and conventional extraction for all the metals in the sediment CRMs are observed when the F2 content is estimated, single extractions provide an efficient extraction only for Cd (Fig. 1) when applied to the soil CRM. The high lability of this element and its main association with manganese oxides would explain Cd behaviour. For the rest of elements, matrix characteristics would account for the lack of extractability in the single extraction. The high carbonate content of BCR 141R, would probably consume an important part of the extractant reagent, being not enough the H⁺ available for completely dissolve the different components that typically are related to reducible fraction (manganese oxides, crystalline and amorphous iron oxyhydroxides).

With a few exceptions (e.g. Pb in BCR 601), single extraction yielded good recoveries in the oxidable fraction. When total extractable contents are compared (sum of F1+F2+F3) (Table 4),

single extractions yielded recoveries in the range 90-110 % for all metals in both sediments. However, as expected, low recoveries for total extractable content (<60%) are achieved with the soil sample except for Cd.

Ultrasonic treatment caused higher metal amounts of Cr, Cu and Zn (BCR 141 R) and Cr and Pb (BCR 601) to be released in F1. Such release enhancement by ultrasonic cavitation is also observed for Fe ($137 \text{ mg}\cdot\text{kg}^{-1}$ against $45 \text{ mg}\cdot\text{kg}^{-1}$ in conventional treatment for BCR 141R) and Mn as a consequence of the related oxides disaggregation and colloid formation (smaller than $0.22 \mu\text{m}$). Thus, the observed increase of metal release can be attributed to the enhancement of the contact interface between metal oxides and extractant. A comparison of F1 in the three CRMs assayed reveals that BCR 701 provided the best results as all metals are efficiently recovered, while for the other two CRMs only two metals are similarly extracted (Cd and Ni in BCR 141R; Cd and Cu in BCR 601). In F2, a general underestimation is observed for Ni due to a clear lack of extraction efficiency by the ultrasonic agitation, also observed in the sediment sample for Cr, another typical residual element. The rest of elements present recoveries around 100%. This is an apparent contradiction because of the relatively different concentrations of the metals released on F1 and F2. In this sense, the lower concentrations of F1 can be highly modified by a slight attack of Fe-Mn oxides. This attack does not modify in a noticeable manner the amounts released on F2. In the oxidable fraction most metal recoveries vary in the range (70-130%). Again, Ni displays lower recovery than that of the conventional procedure. This behaviour is displayed regardless the solid matrix, a fact that is in agreement with previously reported data for Ni using small-scale studies over BCR 601.²³ Sonication conditions different than the optimised should be used in order to efficiently recover this element, but would involve an overestimation of the other elements.²⁴ Finally, total extractable content (sum of F1+F2+F3 contents) (Table 4) with ultrasonic agitation were similar in comparison with the conventional protocol except for Ni (BCR 141R and BCR 601) and Cu (BCR 141R).

Readsorption studies

Added amounts and metal readsorptions (%) for each metal in each CRM for the acid-soluble, reducible and oxidable fraction are shown in Table 5. Repeatability of readsorption values, expressed as RSD, was better than 9%, with exception of Pb in the F1 on BCR 141R where released amounts were close to the LO, hence limiting the readsorption quantification.

Conventional three-stage sequential extraction scheme

On applying the conventional SM&T-SES, readsorption occurs for almost all metals and CRMs in F1. Readsorption is especially highlighted (>90%) in F1 for Cu (BCR 141R) and Pb (BCR 601). Readsorption values in the range 60-90% are observed for [Cr(F1), Cd(F3)] in BCR 701 and [Cu(F1), Cu(F3)] in BCR 601 (Table 5).

Depending on the matrix characteristics and its buffering capacity, a pH increment about 2 pH units is observed in F1 (final pH of 4.8-5). Comparing with the observed increment in the other fractions (only about 0.5 pH units), this aspect would explain the favoured phenomena of readsorption over remaining active surface sites in the iron and manganese oxides. Some metals (e.g. Zn) suffer from readsorption in a similar way than with other SESs, where higher readsorptions are observed when the acid soluble amounts are lower, due to an increase of the number of active sites uncovered in the sample.¹⁴ Another example is the high and well-known readsorption of Pb,²⁵ also observed within the studied CRMs. We then consider that readsorbed metal is redistributed to iron and manganese oxides, what has been elsewhere assessed by means of radiochemical

techniques.²⁶ In contrast, the readsorption phenomena was successfully avoided in F2 as a result of the initial acidic conditions and the poor buffering capacity of the matrix, which prevents the pH to rise, and in turn, readsorption.²⁷ Within the oxidable fraction, soil CRM generally displays a lower readsorption than the sediments. Only Pb and Zn present a low and comparable readsorption for the three CRMs. In CRMs, BCR 601 and 701, the readsorption extent is higher for Cd, Cr, Cu and Ni in comparison with the soil.

Single extractions

Readsorption studies are limited to the reducible and oxidable fractions in the single extractions due to similar operational conditions with respect to the conventional procedure in the acid soluble fraction. In this sense, readsorption trends in the first fraction have been already discussed above. For reducible and oxidable fractions, it would be expected that the unattacked fractions during the single extraction procedure would play an important role in the readsorption studies. In general, it can be appreciated from data shown in Table 5, that the previously untreated acid soluble fraction do not markedly affect the readsorption of metals for BCR 601 and 701 in the reducible fraction, being readsorption values similar to those of the conventional SES.

However, in F2, the single extraction approach suffered from high readsorption in BCR 141R for all metals with exception of Cd, which showed no readsorption. The occurrence of significant amounts of carbonates in the soil CRM should account for this behaviour. Thus, carbonate dissolution should consume most of the acid content in the reducing reagent leading to inefficient dissolution of the Fe-Mn oxides, and in turn, to enhanced readsorption.

When comparing the readsorption extent in the single and conventional extraction for the oxidable fraction, almost no differences are observed for all the CRMs (See Table 5).

On applying single extractions, high readsorption (i.e. 60-90%) was found for Cr(F2), Cu(F2), Ni(F2) on BCR 141R; Cr(F1), Cd(F3) on BCR 701 and Cu(F1) on BCR 601 and severe readsorption (i.e. >90%) observed for Cu(F1) and Pb(F2) on BCR 141R and Pb(F1) on BCR 601

In general, a relationship between the readsorption extent and recovery occurs (see Table 5). Thus, poor recoveries can be observed for Cr(F2), Cu(F2) and Ni(F2) on BCR 141R, which are related with high readsorption.

Ultrasonic extractions

As above, a relationship between recovery and the readsorption extent was observed in many cases. High readsorption (i.e. 60-90%) is observed with Cd(F3), Pb(F3) and Zn(F3) for BCR 141R; Cr(F1), Cu(F1) and Cd(F3) for BCR 701; Cu(F3) for BCR 601. Severe readsorption (i.e. >90%) is observed with Cr(F1), Cu(F1) and Pb(F1) for BCR 601 (Table 5).

In F1, excess extraction occurs for Cr, Cu and Zn (BCR 141R) by implementing ultrasonic agitation in comparison with the conventional SM&T SES, which is correlated with lower readsorption (See Table 5). On the other hand, for Cu (BCR 701) and Ni and Zn (BCR 601) lower recovery can be observed as a result of enhanced readsorption. Apparently, this relationship is less clear for Cd, Cr and Cu (BCR 601), which display better or the same relative extractability with higher readsorption taking place. In these cases, the role of ultrasound activating the remaining surface would enhance readsorption over freshly new exposed active sites. However, increased extraction efficiency caused by the ultrasonic action should operate on the opposite direction yielding higher metal content in the extract. The rest of

metals show similar readsorption percentages as those of the conventional procedure in F1.

While any CRM generally show a comparable readsorption to the conventional procedure in F2 using ultrasonic agitation, an enhanced readsorption takes place for all metals extracted from BCR 141R in F3. Higher readsorption is also observed in this fraction for Cd, Ni, Pb and Zn extracted from BCR 601. Although less easily observed than in the above fractions, diminished relative extractability as a result of increased readsorption is evident (e.g. Ni and Zn from BCR 601) in F3. However, the lower readsorption occurring for Cr and Ni when extracted from BCR 701 using ultrasonic agitation did not result in increased recovery, as could be expected. In both cases, low readsorption in the oxidable fraction could compensate for low extraction efficiency thereby yielding similar recovery.

Conclusions

Readsorption processes are observed with the three approaches employed to obtain information about extractable metal contents in soil and sediments. Readsorption is enhanced for many metals and fractions when ultrasonic agitation by a probe is applied to shorten the extraction time in comparison with the conventional SES, hence indicating the activation of adsorptive sites. The readsorption artefact is particularly critical using the single extraction approach with BCR 141R soil, being enhanced by the presence of unattacked phases owing to reagent exhaustion.

For many metal/fraction pairs, recovery attained with the accelerated methods is related to readsorption. When readsorption for the accelerated method is similar to that of the conventional SM&T SES, recovery approaches 100%. The readsorption phenomena suggest that metal distribution has to be cautiously interpreted, principally that of Cu and Pb due to severe readsorption focused on the acid soluble fraction.

Acknowledgment

This work has been financially supported by Xunta de Galicia (Project PGIDT01PX13101PR). The authors thank the CACTI Laboratory (University of Vigo) for assistance with the atomic emission spectrometer. Financial support from the Universitat Autònoma de Barcelona is also gratefully acknowledged.

References

- 1 A. Tessier, P.G.C. Campbell, and M. Bisson, *Anal. Chem.* 1979, **51**(7), 844.
- 2 A.M. Ure, Ph. Quevauviller, H. Muntau, and B. Giepink, *Intern. J. Environ. Anal. Chem.* 1992, (**51**), 135.
- 3 A.V. Filgueiras, I. Lavilla and C. Bendicho, *J. Environ. Monit.* 2002, **4**, 823.
- 4 F.M.G. Tack, H.A.H. Vossius and M.G. Verloo, *Intern. J. Environ. Anal. Chem.*, 1996, **63** 61.
- 5 I. Ipolyi, C. Brunori, C. Cremisini, P. Fodor, L. Macaluso and R. Morabito, *J. Environ. Monit.*, 2002, **4**, 541.
- 6 B. Pérez Cid, I. Lavilla and C. Bendicho, *Anal. Chim. Acta*, 1998, **360**, 35.
- 7 B. Pérez Cid, I. Lavilla and C. Bendicho, *Intern. J. Environ. Anal. Chem.* 1999, **73**, 79
- 8 C.M. Davidson and G. Delevoye, *J. Environ. Monit.*, 2001, **3**, 398.
- 9 G. M. Greenway and Q. J. Song, *J. Environ. Monit.*, 2002, **4**, 950.
- 10 M. Gulmini, F. Ostacoli, V. Zelano and A. Torazzo, *Analyst*, 1994, **119**, 2075.
- 11 M. Ginepro, M. Gulmini, G. Ostacoli and V. Zelano, *Intern. J. Environ. Anal. Chem.*, 1996, **63**, 147.
- 12 E. Campos, E. Barahona, M. Lachica, and M.D. Mingorance, *Anal. Chim. Acta*, 1998, **369**, 235.
- 13 B. Pérez Cid, I. Lavilla and C. Bendicho, *Anal. Chim. Acta*, 1999, **378**, 201.
- 14 J.L. Gómez-Ariza, I. Giráldez, D. Sánchez-Rodas and E. Morales, *Anal. Chim. Acta*, 1999, **399**, 295.
- 15 C. Kheboian and F. Bauer, *Anal. Chem.*, 1987, **59**, 1417.
- 16 S.O. Ajayi and G.W. Vanloon, *Sci. Total Environ.*, 1989, **87/88**, 171.
- 17 C. Whalley and A. Grant, *Anal. Chim. Acta*, 1994, **291**, 287.
- 18 P.S. Rendell and G. E. Batley, *Environ. Sci. Technol.*, 1980, **14**, 314.
- 19 A. Sahuquillo, J.F. López-Sánchez, R. Rubio, G. Rauret, R.P. Thomas, C. M. Davidson and A.M. Ure, *Anal. Chim. Acta*, 1999, **382**, 317.
- 20 The certification of the total contents (mass fractions) of Cd, Co, Cr, Cu, Hg, Mn, Ni, Pb and Zn and the aqua regia soluble contents (mass fractions) of Cd, Co, Cr, Cu, Hg, Mn, Ni, Pb and Zn in a calcareous loam soil, CRM 141R, European Comission BCR Information Reference Materials, Luxembourg, EUR, 1996.
- 21 The certification of the extractable contents (mass fractions) of Cd, Cr, Cu, Ni, Pb and Zn in freshwater sediment following a sequential extraction procedure BCR-701. European Comission BCR Information Reference Materials, Luxembourg, EUR, 2001.
- 22 The certification of the EDTA-extractable contents (mass fractions) of Cd, Cr, Ni, Pb and Zn in sediment following a three-step sequential extraction procedure CRM 601, European Comission BCR Information Reference Materials, Luxembourg, EUR, 1997.
- 23 A. V. Filgueiras, I. Lavilla and C. Bendicho, *Anal. Bioanal. Chem.*, 2002, **374**, 103.
- 24 B. Pérez-Cid, *Heavy Metals Speciation in Environmental Samples by Means of Sequentially Accelerated Methods of Selective Chemical Extraction*. Thesis. University of Vigo. 1998.
- 25 M. Raksataya, A. G. Landon and N. K. Kim, *Anal. Chim. Acta*, 1996, **332**, 1.
- 26 E. A. Gilmore, G. J. Evans and M.D. Ho, *Anal. Chim. Acta*, 2001, (**539**), 139.
- 27 K. F. Mossop and C. M. Davidson, *Anal. Chim. Acta*, 2003, **478**, 111.

Double Column Figure/Scheme

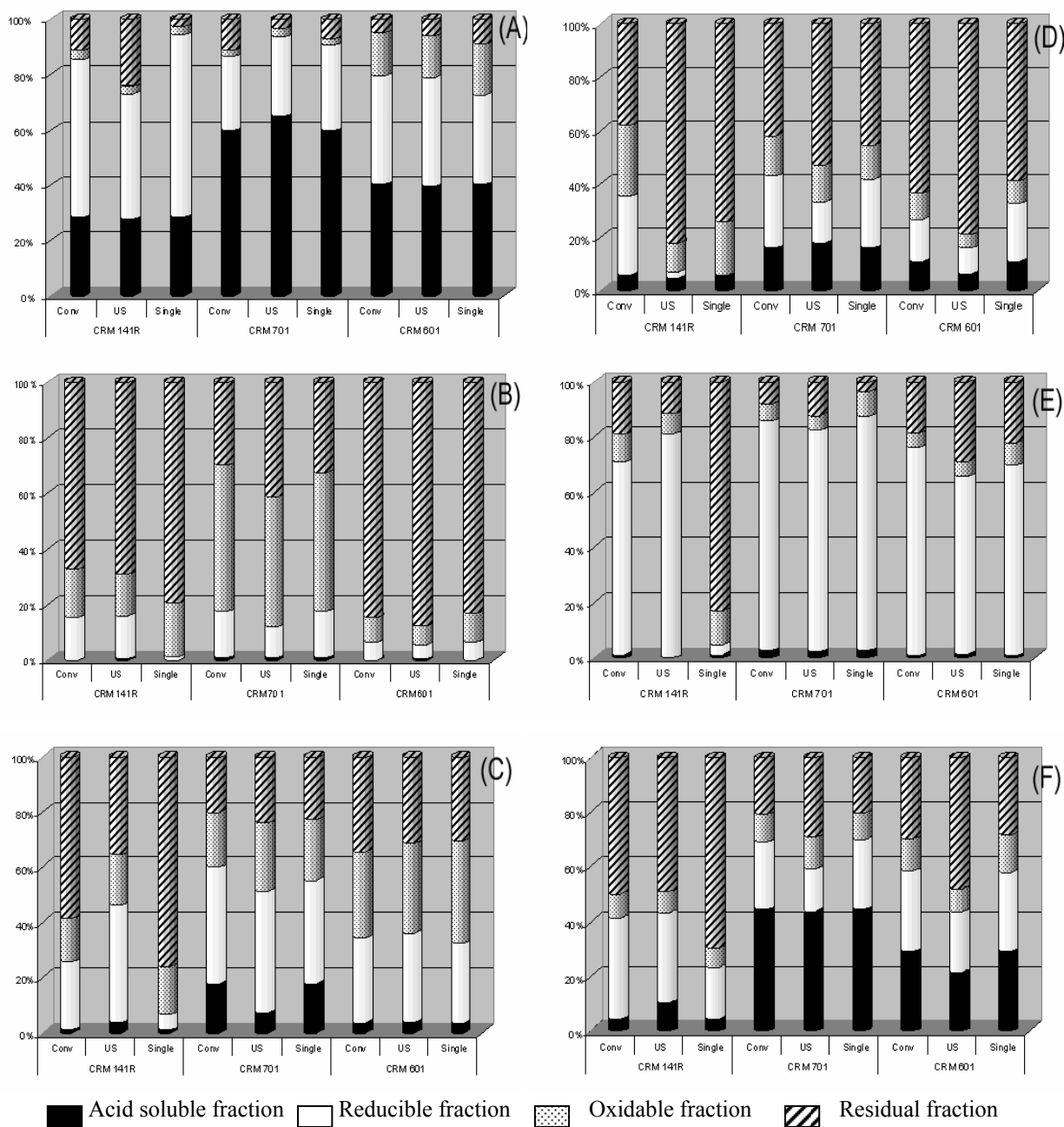


Fig.1 Fractionation patterns of (A) Cd, (B) Cr, (C) Cu, (D) Ni, (E) Pb and (F) Zn in BCRs 601, 701 and 141R when applying the conventional SES (Conv.), single extractions (Single) and ultrasonic extractions (US). (100% represents the sum of the four fractions).

Double Column Table

Table 1 Description of the CRMs examined in this study. Major composition and total trace metals of the CRMs studied.

CRM	Major components (%)								Pseudototal metal (mg·kg ⁻¹)					
	SiO ₂	Al ₂ O ₃	MgO	TiO ₂	Fe ₂ O ₃	P ₂ O ₅	K ₂ O	Organic C (wt.%)	Cd	Cr	Cu	Ni	Pb	Zn
BCR 141R [20] Calcareous loam soil from upper 10cm of fields near Pellegrino, Italy. Ground to < 90 μm.	51.1	11.6	2.3	0.6	4.0	0.4	1.6	11	14.6	195	46.4	103	57.2	283
BCR 701 [21] Lake sediment from different sampling sites of Lake Orta, Italy known for serious metal contamination. Ground to < 90 μm	59.4	15.6	3.2	0.7	6.4	0.5	2.6	10	11.7	272	275	103	143	454
BCR 601 [22] Lake sediment from different sampling sites of Lake Flumendosa, Italy. Collected in March 1994. Ground to < 90 μm.	48.8	13.9	2.2	0.8	7.3	0.9	2.6	5	11	148	240	72	231	824

Table 2 Analytical conditions and chemical reagents for the conventional SES and ultrasonic extractions, both with the *aqua regia* digestion add-on step. The single extraction approach follows the same operational conditions than the conventional SES but over fresh samples in every step. Moisture content of CRMs was determined by drying it at 105 C until constant weight.

Chemical Reagents and conditions			
Step	Fraction	Conventional extraction SM&T-SES	Ultrasonic extraction
1	Acid soluble (F1)	0.5 g of CRM portion, 20 ml 0.11 M acetic acid, shake 16 h. Centrifugation and separate extract from residue at 3000 g for 20 min.	0.5 g of CRM portion, 20 ml 0.11 M acetic acid, 12 min ultrasonic sonication at 50 % amplitude. Centrifugation and separate extract from residue at 3000 g for 20 min.
2	Reducible (F2)	Add 20 ml 0.5 M NH ₂ OH·HCl (pH≈1.5) to step 1 residue, shake 16 h. Centrifugation as in step 1.	Add 20 ml 0.5 M NH ₂ OH·HCl (pH≈1.5) to step 1 residue, ultrasonic sonication during 9 min at 50 % amplitude. Centrifugation as in step 1.
3	Oxidable (F3)	Add 5 ml H ₂ O ₂ pH (2-3) to sep 2 residue digesting at room temperature during 1 h, heat to 85 ± 2 °C for 1 h, add further 5 ml H ₂ O ₂ and heat to 85 ± 2 °C for 1 h; add 25 ml 1 M NH ₄ OAc (pH 2) and shake 16 h. Centrifugation as in step 1.	Add 5 ml H ₂ O ₂ pH (2-3) to sep 2 residue digesting at room temperature during 1 h. Digest with ultrasound during 9 min at 50 % amplitude, heat near dryness and add 25 ml 1 M NH ₄ OAc (pH 2), ultrasonic sonication 6 min at 50 % amplitude. Centrifugation as in step 1.
4	Residual (F4)	Validated microwave-assisted digestion of step 3 residue with 6 ml HCl _{conc} , 2 ml HNO _{3 conc} , 1 ml H ₂ O. Also used for pseudototal digestion of 0.25 g of original CRM using the same acid mixture.	

Table 3 Indicative and experimental extractable concentrations for Cd, Cr, Cu, Ni, Pb and Zn in BCR 601 and 701 CRMs (mg/kg) using the conventional extraction procedure

		F1 (Acid soluble fraction)		F2 (Reducible fraction)		F3 (Oxidable fraction)	
		Determined	Certified	Determined	Certified	Determined	Certified
BCR 701	Cd	7.0 ± 1.5	7.3 ± 0.4	3.1 ± 0.3	3.8 ± 0.3	0.24 ± 0.05	0.27 ± 0.06
	Cr	2.5 ± 0.5	2.26 ± 0.16	45.8 ± 0.8	46 ± 2	142 ± 8	143 ± 7
	Cu	49 ± 3	49.3 ± 1.7	116 ± 5	124 ± 3	55 ± 10	55 ± 4
	Ni	16.7 ± 0.7	15.4 ± 0.9	27.9 ± 0.1	26.6 ± 1.3	15.8 ± 1.1	15.3 ± 0.9
	Pb	3.6 ± 0.5	3.2 ± 0.2	119 ± 4	126 ± 3	11.0 ± 1.5	9 ± 2
	Zn	202 ± 9	205 ± 6	112 ± 3	114 ± 5	45 ± 3	46 ± 4
BCR 601	Cd	4.0 ± 0.7	4.5 ± 0.6	4.0 ± 0.5	3.9 ± 0.5	1.52 ± 0.10	1.91 ± 1.3
	Cr	0.39 ± 0.03	0.35 ± 0.07	10.0 ± 0.5	10.6 ± 0.8	13.5 ± 1.5	14 ± 2
	Cu	9.5 ± 1.0	10.5 ± 0.7	71 ± 2	73 ± 5	75 ± 4	79 ± 8
	Ni	8.3 ± 0.5	7.8 ± 0.8	10.8 ± 1.2	10.6 ± 1.1	6.1 ± 0.7	6.0 ± 1.2
	Pb	2.3 ± 0.6	2.3 ± 0.4	210 ± 4	205 ± 10	17.3 ± 1.3	20 ± 5
	Zn	251 ± 4	261 ± 12	265 ± 3	266 ± 16	107 ± 7	106 ± 10

Table 4 Summary of total extractable content (F1+F2+F3) (mg·kg⁻¹) obtained for BCR 141R, BCR 701 and BCR 601 by conventional SES, single extraction and ultrasonic extraction.

		Cd	Cr	Cu	Ni	Pb	Zn
BCR 141R	Conventional	10.9 ± 1.2	49 ± 2	16.1 ± 1.3	59 ± 5	37 ± 2	144 ± 17
	Single Extraction	11.9 ± 0.5	30.9 ± 0.8	9.5 ± 0.7	24 ± 3	8 ± 3	87 ± 5
	Recovery (%) ^a	110	63	59	41	21	60
	Ultrasound	9.4 ± 0.3	46.9 ± 1.0	25.2 ± 1.7	17.0 ± 1.0	40.4 ± 0.8	146 ± 5
	Recovery (%)	86	95	157	29	109	101
BCR 701	Conventional	10.4 ± 1.5	191 ± 8	220 ± 12	59.9 ± 1.3	132 ± 5	360 ± 10
	Single Extraction	10.8 ± 0.5	187 ± 10	213 ± 8	56.1 ± 0.9	138 ± 5	363 ± 14
	Recovery (%)	105	96	97	94	105	101
	Ultrasound	11.3 ± 0.8	159 ± 5	209 ± 7	48.5 ± 1.5	126 ± 4	322 ± 2
	Recovery (%)	109	83	95	81	95	90
BCR 601	Conventional	9.4 ± 0.3	23.8 ± 0.5	152 ± 3	26.4 ± 0.6	229 ± 16	600 ± 14
	Single Extraction	9.0 ± 0.9	27.8 ± 1.4	162 ± 6	29 ± 2	218 ± 6	614 ± 10
	Recovery (%)	96	108	106	112	95	102
	Ultrasound	9.3 ± 0.7	19.1 ± 0.6	160 ± 7	15.0 ± 0.3	199.7 ± 1.3	445 ± 4
	Recovery (%)	99	80	105	57	87	74

^a Recovery is calculated using the ratio: [total metal content (F1+F2+F3) extracted using the accelerated (single extractions or ultrasonic agitation) procedure/total metal content extracted by the conventional sequential procedure] × 100..

Table 5 Added amounts (μg), readsorption (RA) and recovery (RC) values (%) for metals in the different fractions of SM&T-SES. Conv (Conventional), US (Ultrasound), Single (Single extraction)

CRM		Cd		Cr		Cu		Ni		Pb		Zn		
		(μg)	RA (RC)	(μg)	RA (RC)	(μg)	RA (RC)	(μg)	RA (RC)	(μg)	RA (RC)	(μg)	RA (RC)	
Acid soluble fraction	BCR 141R	Conv	n.s. ^a		27		99		34		n.d. ^b		58	
		Single	0.9	n.s.	0.1	27	0.2	99	1.5	34	-	n.d.	3.2	58
		US		29 (97)		n.s. (311)		60 (405)		53 (82)		n.d.		37 (230)
	BCR 701	Conv		17		83		29		n.s.		54		11
		Single	2.0	17	0.6	83	13	29	4.0	n.s.	0.9	54	55	11
		US		12 (109)		86 (107)		79 (41)		n.s. (110)		55 (78)		10 (99)
	BCR 601	Conv		n.s.		51		82		n.s.		94		29
		Single	1.1	n.s.	0.2	51	2.8	82	2.2	n.s.	0.9	94	56	29
		US		41 (98)		95 (266)		103 (105)		33 (58)		97 (163)		39 (74)
Reducible fraction	BCR 141R	Conv		n.s.		n.s.		n.s.		n.s.		34		18
		Single	1.9	n.s. (116)	6.0	86 (10)	3.0	89 (23)	7.6	72 (0)	8.6	92 (5)	30	30 (51)
		US		25 (80)		12 (101)		42 (171)		11 (72)		20 (116)		10 (89)
	BCR 701	Conv		35		n.s.		24		12		18		12
		Single	1.0	15 (116)	12	13 (101)	32	25 (89)	7.0	n.s. (94)	34	18 (103)	30	12 (104)
		US		17 (108)		8 (68)		52 (105)		n.s. (57)		6 (97)		11 (63)
	BCR 601	Conv		n.s.		n.s.		n.s.		n.s.		n.s.		10
		Single	1.1	n.s. (82)	2.7	n.s. (96)	20	18 (93)	2.9	n.s. (136)	55	n.s. (91)	72	19 (98)
		US		50 (100)		n.s. (78)		n.s. (105)		n.s. (61)		n.s. (86)		13 (75)
Oxidizable fraction	BCR 141R	Conv		n.s.		n.s.		n.s.		n.s.		23		32
		Single	0.1	39 (98)	7.2	n.s. (110)	1.6	n.s. (115)	7.2	n.s. (76)	1.2	31 (130)	7.2	21 (80)
		US		69 (88)		41 (88)		47 (118)		49 (41)		67 (72)		64 (88)
	BCR 701	Conv		79		55		36		49		20		14
		Single	0.2	78 (104)	39	59 (97)	15	41 (94)	4.1	45 (84)	2.4	26 (118)	12	27 (90)
		US		71 (138)		18 (91)		41 (104)		n.s. (89)		34 (71)		n.s. (104)
	BCR 601	Conv		32		55		69		n.s.		17		31
		Single	0.5	26 (119)	3.1	49 (117)	21	51 (119)	1.6	16 (86)	5.4	15 (156)	29	41 (120)
		US		51 (103)		56 (78)		67 (105)		55 (49)		58 (103)		59 (74)

^a n.s.: non-significant readsorption (< 5%). ^b n.d.: not detected, < LOQ. RA: Readsorption (%); RC: Recovery (%). Recovery values are shown between parenthesis.

ANEXO 5

*Comparison of leaching test applied over roadside sediments.
Assessment of heavy metals remobilisation by fractionation.*

G. Pérez, M. Valiente. To be submitted.

Comparison of leaching tests applied over roadside sediments. Assessment of heavy metals remobilisation by fractionation.

G.Pérez, M. Valiente*

*Centre GTS. Unitat de Química Analítica. Departament de Química. Universitat Autònoma de Barcelona. Facultat de Ciències. Edifici CN. 08193. Bellaterra, Barcelona, Spain.
E-mail: Manuel.Valiente@uab.es*

***This submission was created using the RSC Article Template (DO NOT DELETE THIS TEXT)
(LINE INCLUDED FOR SPACING ONLY - DO NOT DELETE THIS TEXT)***

Roadside deposited sediments pollution related to heavy metals (Cd, Cr, Cu, Ni, Pb and Zn) along 20 km of C-58 highway has been assessed by means of several leaching tests. Total, available and bioavailable amounts have been obtained by pseudototal digestion, mild, acid and complexing extractants leaching tests, after applying over 16 samples (three of them related to background soil reference). Additionally, the Standard Measurement and Testing (SM&T), formerly Bureau Community of Reference (BCR), sequential extraction scheme (SES) was performed in order to gain information about heavy metals (HMs) fractionation. From the obtained pseudototal content data an anthropogenic enhancement of Cu, Pb and Zn after considering the concentration enrichment ratio (CER) and environmental concentration guideline values (ECG) is suggested. However, this data can be further refined when considering the additional data obtained from the other leaching tests providing a more realistic environmental situation. Not only the additional information but also the reliability as powerful screening tools have been observed for some single leaching procedures. This help to clear and promptly identify real hazardous areas needing a remedial strategy as those at the middle area of the studied transect of the highway.

Introduction

Within those environmental matrices that have gained concern during last years,¹ roadside sediments are of great interest due to the possible transmission of their pollutant charge to other reservoirs that may constitute a health hazard. High amounts of metals have been detected in these sediments and their origin is linked to the combustion processes of vehicles, road surface degradation, application of road maintenance chemicals such as deicing salts, wearing of vehicles, wearing of signposts and crash barriers.² The pollution proceeding from this sources is emitted in a particulate form and depending on climatic conditions, coarsest particles may accumulate immediately at the asphalt border, mixing with natural components, being sometimes covered by grass, and forming the known as roadside sediments. There is general agreement that the metals pollution decreases in concentration with depth and with distance from the roadway.^{3,4} From the environmental forensics point of view, roadside sediments pollutant charge can be easily characterized and related to non-point source pollution and connected to vehicles emissions, thus acting as environmental registries of valuable information.⁵ Within the considered metals to pollute roadside sediments, those that can be highlighted are Pb proceeding from the combustion of former leaded fuels,⁶ Zn contained in ZnO applied to the rubber compound for tires as a vulcanising agent and also in crash barriers,⁷ Cu as a component found in brake linings and in many alloys and Cd, included in tyres or in lubricating oils that can be spill over due to accidents.⁸

In order to assess the impact of trace elements in soils and sediments not only the total metal content, but also its mobility and bioavailability has to be considered, due to the biogeochemical and ecotoxicological significance of a given contaminant is determined by its specific binding form and coupled reactivity rather than by its total concentration.⁹⁻¹⁰ Consequently, there is a need for information about how easy is their remobilisation depending on their association to sediments, how serious do these metals pose the hazard and if non-point sources can be distinguished from point contamination sources.

In this sense, the use of leaching tests to evaluate labile fractions followed this realization.¹¹

One of the most successful attempts to consider labile fractions and pollutants partition among the different phases presents in soils have been provided by sequential extraction schemes (SEs), also named operationally defined procedures. This methodology is based on the process known as fractionation¹² where a sequential series of selective extractant reagents with an increasing extractant power is employed, in order to selectively dissolve or solubilise the different solid phase forms or mineralogical fractions.¹³⁻¹⁵ In this sense, SEs have become a common evaluative and informative tool giving details on the distribution or partitioning of heavy metals (HMs) in soils and sediments.¹⁶ SEs allow for a better insight into the mechanisms of HMs retention and release involved in the process of migration and decontamination, providing an evaluation of their availability, mobility or persistence.

Simultaneously, single non-selective extractions that target groups of labile or mobile phases have also gained interest, because such an approach can give an useful assessment for screening purposes to identify trace metal pollution,¹⁷ without the hindrance of SEs. Furthermore, these leaching tests present some advantages in front of SEs, mainly related to their cost efficiency, easy to use and a reduction on bias induced by sequential translation and accumulation of procedural errors. Within single extractants and depending on their dissolution power, it is possible to differentiate mild unbuffered extractants, which extract the fraction of easily exchangeable elements, acidic extractants, which release the fraction remobilised by acidification processes and finally the availability promoted by complexing reagents.¹⁸ Leaching tests are focused in the representation of soil-to-plant transfer processes reproducing those chemical reactions that can take place in soils and sediments (e.g. adsorption-desorption, dissolution-precipitation, reduction-oxidation and complexation-decomplexation processes) in a definite specified environment, modifying the concentration of metals in soil solution.¹⁹

The aim of the present study concerns with the characterisation and assessment of the pollution degree of roadside sediments located along 20 km of a crowded Spanish highway (C-58 in Barcelona area). Such characterisation is carried out by both SES and single non-residual extraction of the heavy metals Cd, Cr, Cu, Ni, Pb and Zn. A comparison of the above results has been made to evaluate the distribution of heavy metals between the different soil phases and to throw light on the mentioned transfer processes of these contaminants.

Experimental

Study site, sample collection and processing

The area of interest of this study corresponds to the initial 20 km of C-58 highway close to Barcelona city (Fig. 1). Within this transect, the traffic flow varies in the range of 10,000 to 20,000 vehicles/day (official data by Servei Català de Transit, Generalitat de Catalunya, Spain). A total of thirteen samples representing road deposited sediments alongside C-58 motorway were collected after a long dry period. Additionally, three background samples were collected faraway from possible contamination sources in order to collect soil background data. About 1 kg of each sample was collected by gently sweeping road surface with a clean soft nylon broom, transferring the content of the plastic scoop to a coded polyethylene container and taken to the laboratory. Samples were air-dried (30 °C) during 48 hours and were passed through 2 mm stainless steel sieve to remove large debris. Samples were homogenized by quartering using a riffler. The resulting subsamples were grinded and sieved below 100 µm.

Chemical analyses

In order to evaluate soil matrix effects over pollutants behaviour (i.e. sorption and desorption, distribution etc), soil edaphological parameters were measured, including pH, moisture content (%), organic matter (%O.M.), electrical conductivity (EC), and carbonate content (CO₃%) following the procedures described in the Official Methods of soil analysis envisaged by local governmental regulations (Junta de Residuos, Generalitat de Catalunya, Spain).²⁰ Major components were determined by X-ray fluorescence spectrometry using 56 geological international reference samples for calibration. Samples were diluted (1:40) with lithium tetraborate and melted in a radiofrequency inductive oven to obtain 30 mm diameter pearls. Ranges and average values of sample edaphological characteristics are given in Table 1.

The different single leaching tests were based on the use of mild extractants (CaCl₂, NaNO₃), acid extractants (HAcO and HCl) and complexing reagents (EDTA). Mild extractants aliquots were acidified to prevent growth of bacteria if not immediately analysed. On the other hand, sequential extraction was performed following the 3-steps procedure from Standard Measurements and Testing (SM&T-SES) including the recommended modifications to improve the reproducibility of results.²¹ After each SES step, the suspension was centrifuged and the supernatant separated from the solid phase by filtering with 0.22-micron filter Millex-GS (Millipore, Ireland) to avoid the nebulizer fouling when using ICP-MS or ICP-OES. The resulting extracts were stored in polypropylene bottles at 4 °C prior to analysis, except extracts from the second step, NaNO₃ and CaCl₂, which were analysed immediately due to instability and degradation of the extracting reagent. Treatment for pseudototal metal determination in original samples was the same as that used for residual fraction determination, (i.e. microwave digestion). All extractions and digestions were performed in triplicate including the control of vessel, reagent and procedural blanks. Three different aliquots of each sample were used to determine the moisture content to apply for the

proper correction to dry mass. Table 2 summarizes the experimental conditions applied to the different extractions and digestions.

For a quality control of both measuring conditions and extractions, a mass balance was evaluated by comparison of the pseudototal metal content with the sum of extracted metal percentages when applying the SM&T-SES. Additionally, two different CRMs were employed, including a sewage sludge amended soil (BCR CRM 483)²² with indicative values for CaCl₂, NaNO₃ and the three steps SM&T-SES extractions and certified values for HAcO and EDTA extractions. The second CRM employed was a lake's sediment (BCR 701)²³ with certified values for the SM&T-SES. Prior to the application to sediments samples, single leaching tests and SM&T-SES procedures were validated by means of CRMs, obtaining a good traceability for corresponding HMs in each fraction/extraction (see Table 3). No significant differences were observed (n=3) when applying *F*- and *t*- test.

Apparatus and Reagents

Major components were determined using a Philips PW2400 X-ray spectrophotometer equipped with Rh excitation tubes and a Philips radio-frequency inductive oven (model PERL'X2, Holland). HMs were determined in each extract of the different leaching solutions by using a ThermoElemental inductively coupled plasma optical emission spectrometer (ICP-OES) (model Intrepid II XLS, Franklyn, MA, USA). For trace elements below ICP-OES detection limits, a ThermoElemental inductively coupled plasma mass spectrometer (ICP-MS) (model PQExcell, Windsford, UK) was employed. Quantification of HMs was done using reagent-matched standard solutions, obtained by appropriate dilution of commercial stock solutions (Merck Darmstadt, Germany and J.T. Baker, North Kingstown, RI, USA). Multi-element standard solutions were used for ICP-OES and ICP-MS calibrations. Analytical grade reagents, supplied by either Panreac, Barcelona, Spain, J.T. Baker, Phillipsburg, NJ, USA or Merck, Darmstadt Germany, were used throughout. All glassware and plastic containers were previously soaked overnight in 25% nitric acid and rinsed with double distilled water. Sample digestions for pseudototal determination were performed in perfluoroalcoxy (PFA) vessels, with a CEM Corporation microwave laboratory unit (CEM Mars X, Mathews, NC, USA). Conventional sequential extraction and single leaching tests were performed using a SBS end-over-end mechanical shaker (model ABT-4, Barcelona, Spain). Extracts were separated from solid residues using a Pacisa centrifuge (model C-5, Barcelona, Spain).

Pollution degree assessment

Dutch target and intervention values were taken as reference values to assess the contamination degree of roadside sediments. Three different environmental situations can be depicted from such reference: samples below target, above intervention and between both levels. However, these guidelines are based on total concentrations. Thus, using different leaching extractants, more detailed information can be obtained in terms of mobile or available HMs pollution. Additionally, a better insight of the overall pollution can be obtained by normalizing the different released amounts of HMs to the corresponding Dutch reference levels, thus allowing to plot together the released HMs using different leaching reagents.

Furthermore, complementary reliable information can be obtained by considering the variation of metals concentration within the different geological substrates. In this sense, the proposed evaluation by concentration enrichment ratios (CERs)²⁴ is most appropriate to evaluate the contamination. CERs are calculated considering the concentration of a given element, C_n , in both target sample and background sample,

normalized with respect to a lithogenic conservative element such as Al, which is accurately determined in each sample.

$$CER_n = \frac{\left[\frac{C_n RDS}{C_{Al} RDS} \right]}{\left[\frac{C_n Background}{C_{Al} Background} \right]}$$

The values of CERs allow to differentiate samples by the anthropogenic contribution, being minimal or no anthropogenic enhancement when $CER < 2$, moderate for $2 < CER < 5$, significant when $5 < CER < 20$, very strong for $20 < CER < 40$ and extreme when $40 < CER$.

Results and discussion

Pseudototal content and edaphological characterisation

Characteristic data of roadside sediments can be observed on Table 1. The range of the organic carbon content and electrical conductivity was normal and no significant differences were observed against background samples (non-parametric Mann-Whitney U -test α -level=0.05), while significant higher both carbonate content ($p=0,009$) and pH ($p=0,009$) were observed for roadside sediments. This content will probably arise from the abrasion of the road surface materials and concrete of the basin, which would also explain the high pH of samples as well as their buffering capacity and the related increase on the final pH of the different extractions. With these characteristics, it is expected a certain capability of these sediments to retain dissolved metal ions during road runoff after rainfall episodes.

Establishing the target and intervention Dutch limits as environmental concentration guidelines values, ECG, is possible to rank the different HMs considered when examining the detailed statistical summary of pseudototal content and CERs data in Table 4. In this sense, for the studied samples, Cr and Ni represent those elements with lower impact due to ECG values are below the target value for almost a 75% and 50% of population respectively. Furthermore, the main part of CERs values is distributed below the 10% of population, indicating a minimal or no anthropogenic pollutants enhancement. Only Ni present two samples with a significant and strong anthropogenic apportion.

The other elements represent an anthropogenic implication. From the examined elements, Cd is the less anthropogenically favoured, presenting a general ECG value between target and intervention values. The anthropogenic enrichment is better represented by Cu, Pb and Zn because of a higher number of samples with $CERs > 2$. For Cu it is important to highlight that the half of the samples present values above intervention value reclaiming an urgent remedial strategy. Pb is another clear example of an anthropogenic-enhanced element. Despite leaded fuel was increasingly disused several years ago, 11 samples present CER values between 2 and 20 expressing moderate or significant anthropogenic apportion and a 25 % of the studied samples overcome the intervention value. In the case of Zn, it presents a homogenous distribution with a moderate anthropogenic contribution, with pseudototal contents always below intervention value, except the upper 25% of population. This would suggest the homogeneous tyre and crash barriers degradation along the highway, which are expected to be the main Zn contributors.

Leaching tests

To gain information on mobility and availability of pollutants, the application of single and sequential extraction procedures lead to interpret these parameters for the studied elements in the

considered samples. Results obtained for the roadside sediments and background samples, in which the discussion below is based, are given in Table 5 and 6.

Single extraction efficiency

In general, the released amounts of HMs by mild extractants are below the 2% of the total amount. It is observed the general lower extractant capability of $NaNO_3$ compared to that of $CaCl_2$ for all the metals. In fact, the metal complex formation by chloride anions together with the favoured removal of adsorbed metals cations by Ca^{2+} would explain this fact²⁵⁻²⁶ compared to that involved when Na^+ and NO_3^- ions are implicated in the extraction. It would be expected that those elements typically more available or mobile, such as Zn and Cd, would show this behaviour but the released amounts are only significant for Zn. Released amounts of Pb could be also considered relatively significant. However, the determination of Pb availability by means of mild extractants is known to be limited, due to the contamination of Pb in soils is a process controlled by the precipitation of hydroxides, carbonates, sulphates and phosphates.²⁷

Taking into account the total amount of metals released by the different acidic extractants employed, the relative sequence follows: $HAcO\ 0.11\ mol\ l^{-1} < HAcO\ 0.43\ mol\ l^{-1} < HCl\ 0.5\ mol\ l^{-1}$ due to the increasing acidity, which lead not only to the dissolution of carbonates but also other phases. In this sense, the increase of Pb extraction, mostly absorbed to iron oxides and hydroxides, is a clear example. Furthermore, the less mobile element, Cr, was more sensitive to this increment in acidity than the most mobile elements such as Cd and Zn, what concerns with the release of Cr from other phases.²⁸⁻²⁹ As a result, the order of the individual metal extraction in the above sequence change dramatically and inversely for Pb and Cd in $HAcO\ 0.11\ mol\ l^{-1}$ with respect to that observed in $HAcO\ 0.43\ mol\ l^{-1}$ and $HCl\ 0.5\ mol\ l^{-1}$ where Cd is less released and Pb becoming more extracted.

For EDTA extractions, the complexation capability of the extractant leads to extract all the metals from exchangeable plus carbonates and oxidable fractions. However, a partial degradation of the oxide layer and certain slow degradation of silicate matrices³⁰ suggest a lack of selectivity when considering the available content assessment. It would be expected that Cu and Pb were more sensible to complexation than to acidification processes³¹ because of their high complexation constants with EDTA ($\log K=17.8$ and 18.3 respectively) and their favoured remobilisation from Fe oxides and hydroxides (Fe-EDTA $\log K=25.1$) where Pb and Cu are highly associated. However, from the ratio $HAcO\ 0.43\ mol\ l^{-1}/EDTA$ extracted amounts for these elements, acidification processes slightly predominate over complexation, while for Zn and Cd, acidification clearly predominates over complexation. Such results can be due to the EDTA neutralisation by the high Fe content that will lead to less extractant available for the other metals.

Sequential extraction

Fractionation is not proportional to the total metal content present in sediments; also, sediments with extremely high differences in total metal content may present similar fractionation patterns. From this aspect, it is clear that results from total metal content are not enough for assessing their environmental impact in sediments thus the fractionation of metals must be considered. In general, some trends can be depicted from the obtained fractionation patterns in Fig. 2, such as the main association of Pb with the reducible phase, a Zn equally and major distribution between the first and second fraction, Cu mainly distributed on the reducible and oxidable phases, an unexpected main distribution of Cd on the residual fraction and the typical Cr in this low mobility fraction. In this

sense, those elements presenting a major residual distribution reflect a control by natural geochemical process rather than an anthropogenic enhancement. Thus, CER values reveal this fact with minimal or no anthropogenic disturbance for Cd, Cr and Ni respectively, while Zn and Pb present moderate anthropogenic apporportion and Cu a significant enhancement.

Most mobile and ready bioavailable metals are those released by the first fraction. From the obtained fractionation the favoured Zn release is observed. Taking into consideration that anthropogenic inputs of Zn control the charge of this element in roadside sediments, it is important to environmentally highlight the fact that one-third of the total amount of Zn is released under acidic conditions, overcoming the Dutch target limit, thus requiring without delay some remedial actuation. The rest of elements do not release significant amounts.

However when considering the reducible fraction additionally to Zn, Cu and Pb present significant released amounts that rise above Dutch target limit. In this case, the role of Fe and Mn oxyhydroxides as scavengers of metals involving sorption processes, tend to control their mobility, thus their solubility. The reducible phase has been considered the main sink for anthropogenic Pb inputs in roadside sediments,³² a fact that is also corroborated within our study. Changes of reducing conditions could lead to an easy release of the major part of accumulated Pb in roadside sediments. The observed reducible fraction sorption trend $Pb^{2+} > Zn^{2+} > Cu^{2+}$ for the considered samples have been also found in previous studies applying SES over road and street sediments.³³⁻³⁴

The target limit is again overwhelmed in the oxidable phase by the same considered metals. The known mobility and translocation of Cu, strongly associated with the fate of organic matter, is not as clear as the Pb associated to the reducible fraction. However, the significant distributed amounts along this fraction have to be well thought out because of Cu can be further mobilised due to bacterial activity when sediments receive water from runoff during rainfall events.³³

Those elements presenting a major residual distribution, such as Cr, Ni and Cd would only release substantial amounts under extreme conditions. In this situation, for several cases these HMs would overcome target and intervention Dutch limits. Their distribution would suggest that these elements are bound to primary and secondary minerals, reflecting the geological characteristics and becoming environmentally immobile.

Correlation among extractants

Unless further assessment on contaminants phase association or other purposes different than screening or monitoring were needed, single leach could be useful. In this sense, among the different possible relationship between leaching tests, HCl extraction procedure reveals similar information to that obtained when using the SES, giving an idea of the total available amounts of HMs under acidic, reducible and oxidable conditions³² and improving the time consuming drawback of SES.

Considering the general positively skewed data for the anthropogenic enhanced HMs (Cu, Pb and Zn), thus the non-normal data distribution and the consequently needed \log_{10} transformation, the regression of the transformed data was statistically significant at $p < 0,001$ with the coefficient of determination shown on Fig. 3, for 13 roadside sediment samples. This suggest that the leached amounts of Cu, Pb and Zn agree with data provided by the overall available amounts ($\Sigma F1, F2, F3$) released by the SES procedure, therefore show the real utility as a fast screening leaching test of HCl procedure.

Distribution of pollutants

From the leaching test data, a more correct assessment on the pollutants availability alongside the highway can be obtained than when using pseudototal content data. This information identifies hazardous points needing remedial strategies. In this sense, plots in Fig. 4, where the ratio between the extracted amounts of anthropogenic enhanced HMs and the Dutch target value are represented, illustrate a reduction on the hazard that represent the different samples. This reduction would depend on the selected level of reference for risk assessment delimited by the employed leaching extractant conditions. Mild extractants are not considered within these representations due to the low extracted amounts and the fact that their normalisation would give a constant value below the target limit.

From the studied samples, and considering those elements that reflect a clear anthropogenic enhancement such as Cu, Pb and Zn, data reveal the greatest ratio for pseudototal content (F4) for Zn (M9, M3, M11 and M7), Cu (M11 and M6) and Pb (M1, M2, M3 and M11). This trend is also observed for Zn and Pb when dealing with less acidic extractants but with a general ratio decrease. This decrease reveals a potential pollution only for Zn in some samples as the rest of values for Cu, Pb and Zn are below or close to the target value. However, for more acidic extractants, normalised values still remain between target and intervention values (which would be 4-5 times the normalised target value, dotted line), suggesting that further investigation or restrictions may be warranted. Moreover, some samples overcome the intervention value; consequently it reveals the need for a remedial strategy.

Further information can be depicted when considering the released amounts under different environmental conditions represented by SES. Thus, Fig. 5 presents data from SES and HCl single leaching test for Cu, Pb and Zn amounts normalised again with respect to Dutch target limit. In this case, reducing environmental conditions represent the worst situation, especially for Pb, where the ratio for F1 and F3 contents are close to target value while F2 contents are the main contribution to the overall available amount and with ratios above the target value, even above the intervention value for sample M3. Zn behaves in a similar way to Pb but only samples M1 and M11, close to the most polluted area, reflect a significant ratio above target limit but always below intervention limits. The case of Cu reflects the major availability of this component under oxidizing conditions, especially for those samples with higher pollution, interpreted as the overall available pollution.

It would be expected a correlation among pollutants concentration and traffic density, with an increasing content in the final sampling area but this was not observed. In fact, samples M3 and M11 with a lower traffic density are those more polluted. The continuous traffic retention accumulated during a whole year of road works, which involve stop and go traffic, road maintenance and frequent accidents would explain the contamination of these samples if compared with initial or final sampling points of the considered area, where a more fluent, despite dense traffic is frequent. Furthermore, the long dry period occurred before the sampling would lead to an ageing and accumulation of pollutants over the roadside sediments. Additionally, the abnormal enriched Zn sampling point at the initial part of the highway would be related to a highway exit with high truck traffic towards the closer industrial areas.

Conclusions

The combination of data provided by pseudototal content and the evaluation of ECGs and CERs, those elements anthropogenically enhanced can be clearly identified. In order to ascertain the degree of overestimation when assessing HMs pollution,

different quick leaching test have been applied. Bearing in mind that acidification procedures predominate over complexation within the considered samples, the comparison between acid leaching extractants once normalised show a significant pollution due to Cu, Pb and Zn with common ECG values between target and intervention values.

Within the different acid leaching tests, HCl procedure can be a suitable, quick and efficient screening tool for HMs pollution assessment, giving reliable information on overall labile phases comparable to that obtained by SES for anthropogenic enhanced HMs, but without the fractionation information. In contrast, mild extractants have been observed to be limited in terms of information provided to high polluted samples due to the low released amounts. In fact, CaCl₂ procedure would be preferred rather than NaNO₃, in terms of risk assessment because of its higher leaching capacity. In this sense, the soil-to-plant transfer process is no significant within the considered samples and the involved metal concentrations released are far below the environmental policy limits.

The acquired data could be used as a baseline database for future studies of the area giving assessment on pollutants accumulation when monitoring studies will be performed by single leaching tests. From the obtained data, urgent actuation is needed close to M3 and M11 sampling area and by simply sweeping thoroughly the area, the hazard could be greatly reduced.

Acknowledgments

Financial support for this study was provided by a research Grant of the Spanish Ministry for Education and Science (PPQ2002-04267-C03-01). The Universitat Autònoma of Barcelona is acknowledged because of the scholarship provided to Gustavo Pérez to perform his PhD studies.

References

- R.A., Sutherland, F.M.G., Tack, C.A., Tolosa and M.G., Verloo, *J. Environ. Qual.*, 2000, **29**, 1431.
- H.D., Van Bohemen and W.H., Janssen Van de Laak, *Environ. Manage.*, 2003, **31**(1), 50.
- N.L., Ward, R.R., Brooks, E., Roberts and C.R., Boswell, *Environ. Sci. Technol.*, 1977, **11**, 917.
- P.K., Lee, J.C., Touray, P., Baillif and J.P., Ildefonse, *Sci. Total Environ.*, 1997, **201**, 1.
- R.A., Sutherland, *Environ. Pollut.*, 2003, **121**, 229.
- J. O., Nriagu, *Sci.Total Environ.*, 1990, **92**, 13.
- E., Smolders and F., Debryse, *Environ. Sci. Technol.*, 2002, **36**, 3706.
- J.V., Lagerwerff and A.W. Specht, *Environ. Sci. Technol.*, 1970, **4**(7), 583.
- M., Kersten, and U., Förstner, in *Trace Element Speciation: Analytical Methods and Problems*, ed. G.E., Batley, CRC Press, Boca Raton, FL, 1989, pp. 245-317.
- W. F., Pickering, in *Chemical Speciation in the Environment*, eds. A.M., Ure and C.M., Davidson, Blackie Academic and Professional, Glasgow, 1995, pp. 9-32.
- V.H., Kennedy, A.L., Sánchez, H.D., Oughton and A.P. Rowland, *Analyst*, 1997, **122**, 89R.
- D.M., Templeton, F., Ariese, R., Cornelis, L.G., Danielsson, H., Mutuau, H.P., Van Leeuwen and R., Lobinski, *Pure Appl. Chem.*, 2000, **72** (8), 1453.
- G., Rauret, *Talanta*, 1998, **46**, 449.
- K., Das, R., Chakraborty, M.L., Cervera and M., de la Guardia, *Talanta*, 1995, **42**, 1007.
- F.M.G., Tack and N.G., Verloo, *Int. J. Environ. Anal. Chem.*, 1995, **59**, 225.
- A.V., Filgueiras, I., Lavilla and C., Bendicho, *J. Environ. Monit.* 2002, **4**, 823.
- R., Chester, W.M., Kudoja, A., Thomas and J., Thomas, *Environ. Pollut. (B)*, 1985, **10**, 213.
- H., Agemian and A.S.Y., Chau, *Arch. Environ. Contam. Toxicol.*, 1977, **6**, 69.
- A., Sahuquillo, A., Rigol and G., Rauret, *J. Environ. Monit.*, 2002, **4**, 1003.
- Departament de Medi Ambient, Junta de Residus, Generalitat de Catalunya, *Pautes d'anàlisi*, Servei de Publicacions, Barcelona, Spain, 1998.
- A., Sahuquillo, J.F., López-Sánchez, R., Rubio, G., Rauret, R.P., Thomas, C.M., Davidson and A.M., Ure, *Anal. Chim. Acta*, 1999, **382**, 317.
- Ph., Quevauviller, G., Rauret, A., Ure, J., Bacon and H. Muntau, *The certification of the EDTA and acetic acid-extractable contents (mass fractions) of Cd, Cr, Cu, Ni, Pb and Zn in sewage sludge amended soils. CRMs 483 and 484*. European Commission BCR Information Reference Materials, Luxembourg, EUR, 1997.
- G., Rauret, J.F., López-Sánchez, D., Lück, M., Yli-Halla, H., Muntau, and Ph., Quevauviller, *The certification of the extractable contents (mass fractions) of Cd, Cr, Cu, Ni, Pb and Zn in freshwater sediment following a sequential extraction procedure BCR-701*. European Commission BCR Information Reference Materials, Luxembourg, EUR, 2001.
- R.A., Sutherland and C.A., Tolosa, *Environ. Pollut.*, 2000, **110**, 483.
- A., Lebourg, T., Sterckeman, T., Ciesielski and H., Proix, *J. Environ. Qual.*, 1998, **27**, 584.
- S.K., Gupta and C.F., Aten, *Int. J. Environ. Anal. Chem.*, 1993, **51**, 25.
- A., Lebourg, T., Sterckeman, T., Ciesielski and N., Gómez, *Environ. Technol.*, 1998, **19**, 243.
- R.W., Peters and L. Sherm, in *Metal Speciation and Contamination of Soil*, eds. H.E., Allen, C.P., Bailey and A.R., Bowers, Lewis Publishers, Boca Raton, FL, 1995, pp. 255-274.
- M., Pueyo, J.F., López-Sánchez and G., Rauret, *Anal. Chim. Acta*, 2004, **504**, 217.
- A., Barona, I., Aranguiz and A., Elias, *Environ. Pollut.*, 2001, **113**, 79.
- A., Sahuquillo, A., Rigol and G. Rauret, *TrAC, Trends Anal. Chem.*, 2003, **22**(3), 152.
- R.A., Sutherland and F.M.G., Tack, *Sci. Total Environ.*, 2000, **256**, 103.
- M., Stone and J., Marsalek, *Water, Air Soil Pollut.*, 1996, **87**, 149.
- M.J., Gibson and J.G., Farmer, *Sci.Total Environ.*, 1984, **33**, 49.

Single Column Figure/Scheme



Fig.1 Map of the studied area. Black line highlights the studied section of C-58 highway localized in the metropolitan area of Barcelona, Spain.

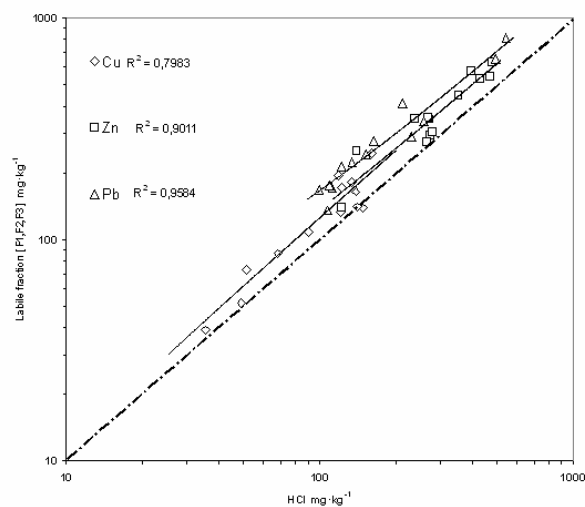


Fig.3 Regression plots between released amounts of HCl single leaching test and overall labile amounts (sum of three fractions of SES) for Cu, Pb and Zn in 13 roadside sediment samples.

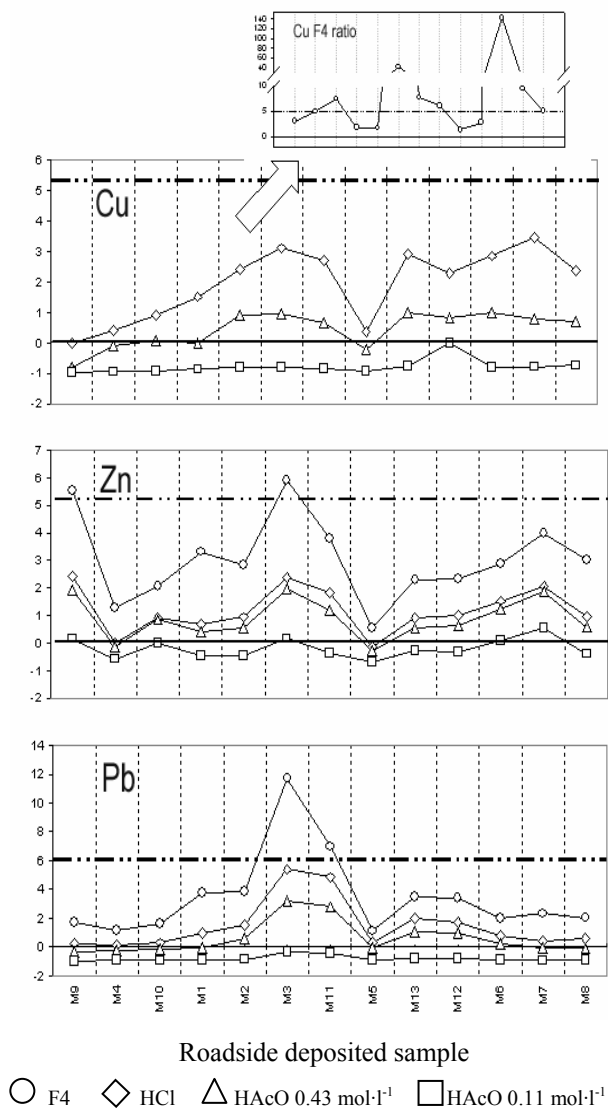


Fig.4 Normalised plot of different acid leached amounts of Cu, Pb and Zn with respect to Dutch target limit. (Full line represents target value, dotted line the intervention value).

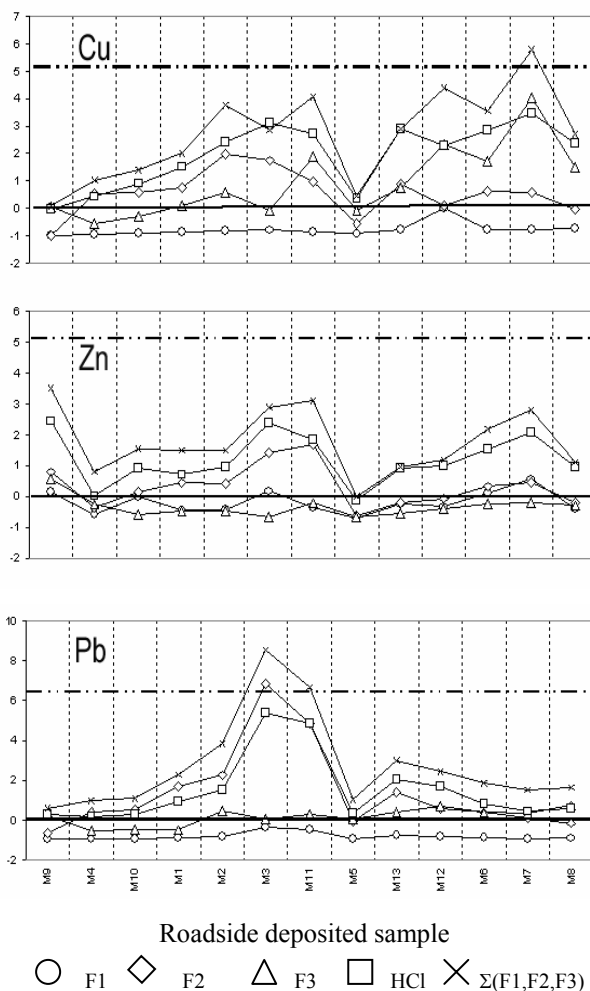


Fig.5 Normalised plot of different leached amounts of Cu, Pb and Zn under different environmental conditions represented by SES steps plus HCl leached amount with respect to Dutch target limit. (Full line represents target value, dotted line the intervention value).

Double Column Figure/Scheme

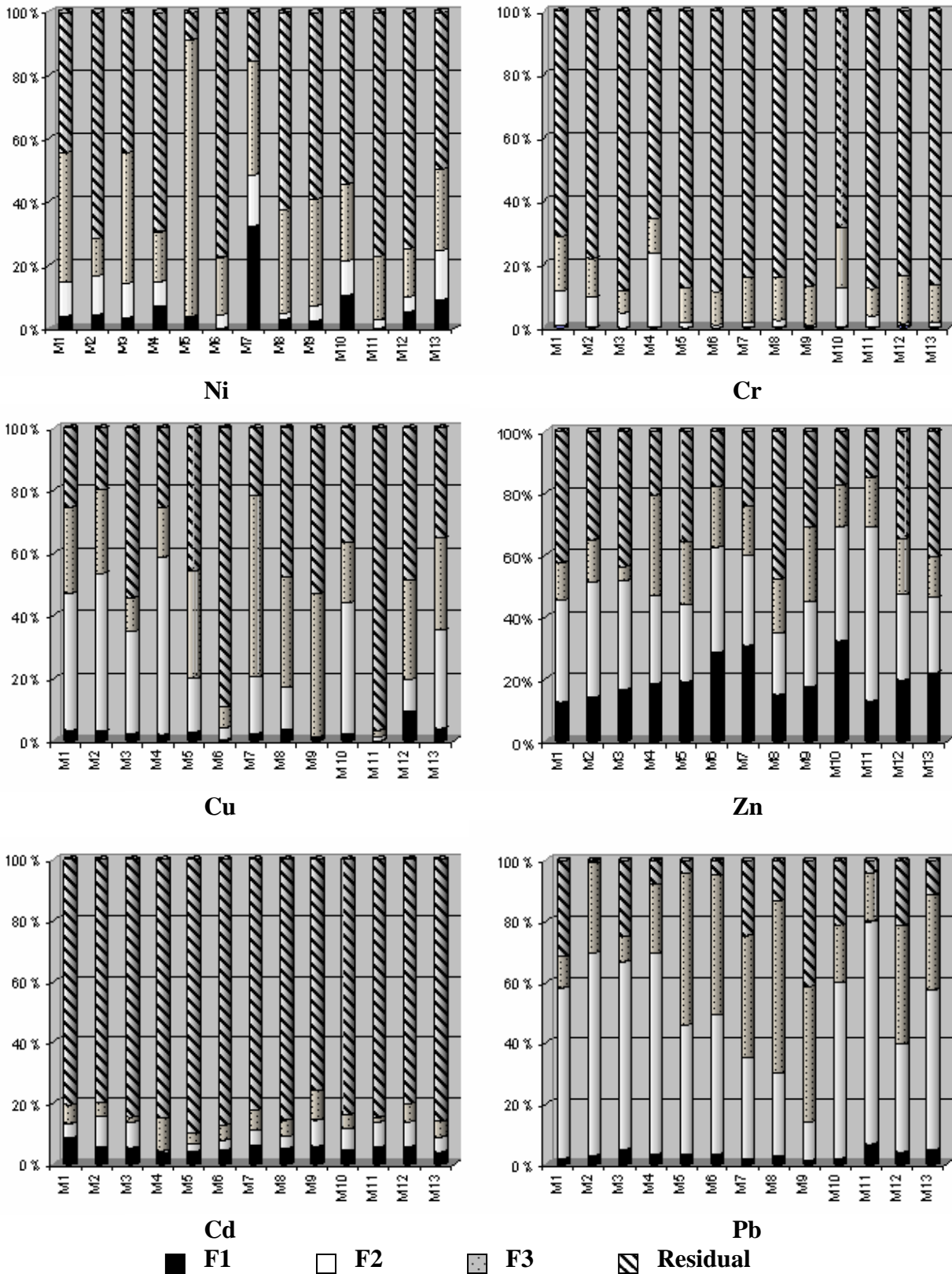


Fig.2 Fractionation patterns of Cd, Cr, Cu, Ni, Pb and Zn in 13 roadside sediment samples. F1, First fraction or adsorbed-exchangeable carbonate phase, F2, Second fraction or reducible phase, F3 Third fraction or oxidizable phase, F4 Fourth fraction or residual fraction.

Single Column Table

Table 1 Statistical summary of mean, maximum and minimum values of edaphological parameters of 13 samples collected along C-58 highway and 3 background samples.

	Background samples	Roadside sediments
pH (potential/total)	7.4 ± 0.1 (7.2-7.6)	8.8 ± 0.2 (8.2-9.4)
Conductivity (mS·dm ⁻¹)	360 ± 45 (315-405)	325 ± 94 (140-678)
Moisture content (%)	0.032 ± 0.005 (0.03-0.04)	0.041 ± 0.007 (0.02-0.06)
Organic mater content (%)	0.6 ± 0.2 (0.3-1.1)	0.7 ± 0.2 (0.2-1.5)
Carbonate content (%)	1.8 ± 0.3 (1.2-2.2)	14.7 ± 1.4 (10.9-17.8)
Major Components (%)		
SiO ₂	36 ± 5 (34.3-38.7)	40 ± 3 (46-30)
Al ₂ O ₃	7.2 ± 0.8 (6.8-7.5)	10.9 ± 0.7 (9.0-12.5)
Fe ₂ O ₃	5.5 ± 0.4 (5.3-5.7)	6.0 ± 0.4 (4.7-7.0)
CaO	20 ± 3 (19.2-21.6)	24.3 ± 1.9 (20.2-29.4)
MgO	1.8 ± 0.3 (1.7-1.9)	1.8 ± 0.3 (1.5-2.2)
K ₂ O	1.5 ± 0.2 (1.4-1.6)	1.7 ± 0.2 (1.4-1.9)
TiO ₂	0.30 ± 0.06 (0.27-0.32)	0.34 ± 0.05 (0.29-0.46)
P ₂ O ₅	0.053 ± 0.020 (0.046-0.063)	0.070 ± 0.012 (0.054-0.086)

Double Column Table

Table 2 Definition of fractions and extraction conditions related to the different leaching and digestions employed tests.

Conditions	Single extractions					Sequential Extractions				Residual
						F1 ^a	F2 ^b	F3 ^c		
Extractant	0,01 mol·l ⁻¹ CaCl ₂	0,1 mol·l ⁻¹ NaNO ₃	0,43 mol·l ⁻¹ HAcO	0,05 mol·l ⁻¹ EDTA	0,5 mol·l ⁻¹ HCl	0,11 mol·l ⁻¹ HAcO	0,5 mol·l ⁻¹ NH ₂ OH·HCl	(a) 8,8 mol·l ⁻¹ H ₂ O ₂ (b) 1.0 mol·l ⁻¹ NH ₄ AcO	37 % HCl 70 % HNO ₃	
pH	-	-	-	-	-	2,85	1,50	2,00	-	
Ratio g:ml	1:10	1:2,5	1:40	1:10	1:20	1:40	1:40	(a) 1:10 (b) 1:50	0.25:10	
Contact Time (h)	2	2	16	1	1	16	16	(a) 2 (b) 16	≈ 0.25	
Agitation	End over end rotation							(a) Digestion 85 C ^d (b) End over end rotation	Microwave digestion with magnetic sitring	
Speed (rpm)	30	120	30	30	30	30-45	30-45	30-45	-	
Liquid separation	Centrifugation + filtration									
Additional steps	-	-	-	-	-	Wash residue before next setp. 1:20, 15 min, additional centrifugation			Pre-digestion 1 hour	

^a Exchangeable, water and acid soluble fraction, ^b Reducible fraction, ^c Oxidable fraction, ^d Predigestion step a t room temperature 1 h.

Table 3 Indicative, certified and experimental extracted amounts for Cd, Cr, Cu, Ni, Pb and Zn values using the 3-steps SM&T-SES and single extractants for BCRs 483 and 701 certified reference materials. (mg·kg⁻¹)

CRM Extraction/Step		Cd	Cr	Cu	Ni	Pb	Zn	
BCR 701	F1	Experimental	7.0 ± 1.5	2.5 ± 0.5	49 ± 4	16.7 ± 0.7	3.6 ± 0.5	202 ± 9
		Certified	7.3 ± 0.4	2.26 ± 0.16	49.3 ± 1.7	15.4 ± 0.9	3.2 ± 0.2	205 ± 6
	F2	Experimental	3.2 ± 0.3	45.8 ± 0.8	116 ± 5	27.9 ± 0.1	119 ± 4	112 ± 3
		Certified	3.8 ± 0.3	45.7 ± 2.0	124 ± 3	26.6 ± 1.3	126 ± 3	114 ± 5
	F3	Experimental	0.24 ± 0.05	142 ± 8	55 ± 10	15.8 ± 1.1	11 ± 2	45 ± 3
		Certified	0.27 ± 0.06	143 ± 7	55 ± 4	15.3 ± 0.9	9 ± 2	46 ± 4
BCR 483	F1	Experimental	10.0 ± 0.77	9.4 ± 3.5	16.8 ± 1.5	17.9 ± 2.0	0.76 ± 0.70	441 ± 39
		Indicative ^a	0.45 ± 0.05	0.35 ± 0.09	1.2 ± 0.4	1.4 ± 0.2	< 0.06	8.3 ± 0.7
	F2	Experimental	24.8 ± 2.3	654 ± 108	141 ± 20	24.4 ± 3.3	379 ± 21	438 ± 56
		Indicative	0.08 ± 0.03	0.30 ± 0.07	0.89 ± 0.22	0.65 ± 0.07	< 0.03	2.7 ± 0.8
	F3	Experimental	1.22 ± 0.48	2215 ± 494	132 ± 29	5.9 ± 1.4	66.5 ± 22	37.1 ± 9.9
		Indicative	18.3 ± 0.6	18.7 ± 0.9	33.4 ± 1.6	25.8 ± 0.9	2.1 ± 0.2	620 ± 23
	CaCl ₂	Experimental	0.47 ± 0.02	0.39 ± 0.06	1.17 ± 0.08	1.42 ± 0.08	0.070 ± 0.008	8.4 ± 0.4
		Indicative	0.45 ± 0.05	0.35 ± 0.09	1.2 ± 0.4	1.4 ± 0.2	< 0.06	8.3 ± 0.7
	NaNO ₃	Experimental	0.11 ± 0.02	0.29 ± 0.07	0.89 ± 0.16	0.60 ± 0.07	0.055 ± 0.007	2.4 ± 0.2
		Indicative	0.08 ± 0.03	0.30 ± 0.07	0.9 ± 0.16	0.65 ± 0.07	< 0.03	2.7 ± 0.8
	HAcO 0.43 M	Experimental	17.7 ± 0.3	18.1 ± 0.4	32.6 ± 0.5	25.0 ± 0.4	2.27 ± 0.06	628 ± 11
		Certified	18.3 ± 0.6	18.7 ± 1.0	33.5 ± 1.6	25.8 ± 1.0	2.1 ± 0.3	620 ± 24
EDTA	Experimental	25.1 ± 1.2	28.9 ± 1.8	208 ± 5	29.4 ± 0.8	223 ± 2	624 ± 4	
	Certified	24.3 ± 1.3	29 ± 3	215 ± 11	28.7 ± 1.7	229 ± 8	612 ± 19	

Results are expressed as the mean of three determinations ± standard deviation. ^a Indicative values obtained from BCR 483 certificate.

Table 5 Summary of extractable metal mean concentrations using sequential extraction scheme in the studied roadside deposited sediment and background samples. (RDS, roadside deposited sediment; Bkgrd, background sample). (mg·kg⁻¹)

Cd	F1		F2		F3		Residual		
	RDS	Bkgrd	RDS	Bkgrd	RDS	Bkgrd	RDS	Bkgrd	
Mean	0.4 ± 0.2	0.11 ± 0.06	0.30 ± 0.02	0.12 ± 0.07	0.24 ± 0.02	0.11 ± 0.06	4.1 ± 0.3	1.7 ± 0.4	
(Max-Min)	0.2-0.9	0.05-0.16	0.03-0.76	0.06-0.18	0.12-0.45	0.05-0.16	3.0-7.8	0.8-2.5	
Cr	Mean	0.37 ± 0.04	0.16 ± 0.04	5.5 ± 0.2	3.7 ± 0.8	12.2 ± 0.3	8.3 ± 1.5	86 ± 6	54 ± 5
(Max-Min)	0.03-1.10	0.13-0.20	0.3-16.5	3.1-4.5	7.4-17.0	6.8-10.0	46-184	44-65	
Cu	Mean	13.0 ± 0.7	2.6 ± 0.2	55 ± 3	22.8 ± 1.8	69 ± 2	24 ± 2	533 ± 99	42 ± 3
(Max-Min)	1.0-60.0	2.5-2.9	0.6-107	21.6-24.8	15-181	23-26	24-4996	40-46	
Ni	Mean	4.1 ± 0.3	1.7 ± 0.6	6.9 ± 0.2	2.0 ± 0.7	35.4 ± 0.9	8 ± 2	117 ± 17	14.1 ± 1.6
(Max-Min)	1.4-19.8	1.3-2.3	0.02-36.8	1.6-2.8	3.3-257.1	6-11	2-977	1.1-1.9	
Pb	Mean	15.4 ± 1.0	1.9 ± 0.3	203 ± 5	28 ± 5	98 ± 5	18 ± 3	64 ± 3	9.4 ± 1.7
(Max-Min)	3.6-56.0	1.6-2.3	29-668	23-32	41-146	15-21	3-270	7.6-10.5	
Zn	Mean	184 ± 6	35 ± 3	185 ± 6	55 ± 5	90 ± 8	30 ± 3	181 ± 12	55 ± 5
(Max-Min)	68-353	33-38	54-377	52-60	44-220	28-32	65-422	51-59	

Table 6 Summary of extractable metal mean concentrations using single leaching extractants in the studied roadside deposited sediment and background samples. (RDS, roadside deposited sediment; Bkgrd, background sample). ($\text{mg}\cdot\text{kg}^{-1}$)

	CaCl_2		NaNO_3		HAcO		EDTA		HCl	
	RDS	Bkgrd	RDS	Bkgrd	RDS	Bkgrd	RDS	Bkgrd	RDS	Bkgrd
Cd										
Mean	8.6 ± 0.8^a	1.4 ± 0.2	BDL ^b	BDL	0.46 ± 0.04	0.26 ± 0.02	0.25 ± 0.02	0.05 ± 0.02	0.57 ± 0.03	0.18 ± 0.02
(Max-Min)	3.6-14.3 ^a	1.2-1.6	-	-	0.26-0.90	0.24-0.28	0.12-0.50	0.03-0.07	0.33-0.96	0.16-0.20
Cr										
Mean	36 ± 3^a	4.20 ± 0.02	BDL	BDL	3.1 ± 0.2	0.13 ± 0.03	0.32 ± 0.01	0.06 ± 0.02	7.3 ± 0.2	5.2 ± 0.2
(Max-Min)	12-83 ^a	4.18-4.21	-	-	0.8-10.1	0.10-0.16	0.22-0.56	0.04-0.08	2.7-11.1	5.0-5.4
Cu										
Mean	0.83 ± 0.07	0.06 ± 0.02	35 ± 3^a	BDL	52 ± 3	11.8 ± 0.2	39 ± 2	2.6 ± 0.3	106 ± 4	38 ± 3
(Max-Min)	0.30-1.95	0.04-0.08	13-83 ^a	-	7-72	11.6-12.0	15-67	2.3-2.8	35-160	35-41
Ni										
Mean	1.3 ± 0.2	0.52 ± 0.08	68 ± 8^a	BDL	5.4 ± 0.5	4.5 ± 0.3	1.1 ± 0.1	0.44 ± 0.03	5.4 ± 0.6	2.1 ± 0.3
(Max-Min)	0.1-3.3	0.44-0.59	6-166 ^a	-	1.7-16.4	4.2-4.8	0.4-1.8	0.41-0.47	2.9-8.8	1.8-2.1
Pb										
Mean	1.5 ± 0.2	0.25 ± 0.03	68 ± 8^a	30 ± 5^a	136 ± 5	66 ± 4	106 ± 3	21 ± 2	211 ± 4	16.3 ± 1.7
(Max-Min)	0.1-3.3	0.22-0.27	7-155 ^a	26-34 ^a	56-354	62-70	50-313	19-23	99-544	14.8-17.8
Zn										
Mean	5.8 ± 0.2	0.8 ± 0.3	369 ± 12^a	116 ± 12^a	261 ± 6	60 ± 6	100 ± 2	24 ± 2	307 ± 5	85 ± 4
(Max-Min)	4.3-8.3	0.5-1.1	273-525 ^a	105-127 ^a	101-415	55-65	46-190	22-26	122-481	81-89

^a $\mu\text{g}\cdot\text{kg}^{-1}$

^b Below detection limit

Table 4 Statistical summary of pseudototal content, CER values, coded environmental concentration guidelines values (ECG) and number of samples per CER class for Cd, Cr, Cu, Ni, Pb and Zn in 13 samples of roadside deposited sediments from C-58 highway.

	Target	Intervention	Min				P ₂₅ ^a				P ₅₀				P ₇₅				Max			
			mg·kg ⁻¹	CER	ECG	CER < 2	mg·kg ⁻¹	CER	ECG	2 < CER < 5	mg·kg ⁻¹	CER	ECG	5 < CER < 20	mg·kg ⁻¹	CER	ECG	20 < CER < 40	mg·kg ⁻¹	CER	ECG	40 < CER
Cd	0.8	12	3.42	0.7	b ^b	8	4.15	1.35	b	5	4.46	1.77	b	0	4.68	2.34	b	0	9.3	3.4	b	0
Cr	100	380	60	0.37	a	12	71	0.84	a	1	88	1.15	a	0	117	1.48	b	0	208	2.24	b	0
Cu	36	190	83	0.37	b	7	135	0.96	b	4	216	1.64	c	1	312	2.25	c	0	5178	42	c	1
Ni	35	210	21	0.27	a	11	32	0.87	a	0	36	1.16	b	1	38	1.25	b	1	1273	65	c	0
Pb	85	350	179	1.12	b	2	231	3.08	b	6	283	4.13	b	5	407	6.62	b	0	1082	9.06	c	0
Zn	140	720	218	0.61	b	3	461	2.01	b	10	542	2.55	b	0	674	2.89	b	0	966	4.84	c	0

^aP₂₅, P₅₀, P₇₅ represent the 25th, 50th and 75th percentiles of the data distributions.

^bECG Values: (a) < TL, below Dutch target limit; TL < (b) < IL, between Dutch target and intervention limits; (c) > IL, above Dutch intervention limit

ANEXO 6

SENSPOL Technical Meeting, Sevilla. Proceedings

M. Valiente, G. Pérez, X. Gaona, D. van Ree, S. Alcock. Cranfield University 2004.

SENSPOL TECHNICAL MEETING, SEVILLA

PROCEEDINGS

Editors:

Manuel Valiente¹, Gustavo Perez¹, Xavi Gaona¹,
Derk van Ree² and Susan Alcock³



1. Universitat Autònoma de Barcelona, Química Analítica, Centre GTS, 08193 Bellaterra (Barcelona), Spain. Manuel.Valiente@uab.es
2. Geodelft. The Netherlands. C.C.D.F.vanRee@GeoDelft.nl
3. Cranfield University, Bedfordshire, UK. s.alcock@cranfield.ac.uk



SENSPOL TECHNICAL MEETING, SEVILLA PROCEEDINGS

Editors:

Manuel Valiente¹, Gustavo Perez¹, Xavi Gaona¹, Derk van Ree² and Susan Alcock³

- ¹. Universitat Autònoma de Barcelona, Química Analítica, Centre GTS, 08193 Bellaterra (Barcelona), Spain. Manuel.Valiente@uab.es
- ². Geodelft. The Netherlands. C.C.D.F.vanRee@GeoDelft.nl
- ³. Cranfield University, Bedfordshire, UK. s.alcock@cranfield.ac.uk

INDEX

1. Summary	4
2. Introduction	6
SENSPOL and DIMDESMOTOM aims	6
Previous Technical Meetings	6
Purpose of the Sevilla Technical Meeting	7
Site description	9
3. Organisation of the Technical Meeting	10
Invitation to participate	10
Preliminary site visit and sampling	10
Chemical analysis	10
Structure of the Technical Meeting	10
Video/DVD	11
4. Description of Instruments	11
5. Results and Discussion	14
Comparison of sensor device capabilities	16
Evaluation of instruments	16
Development stages	16
Calibration	16
Sample preparation requirements	16
Analytical performance	17
Comments on individual instruments	17
- Chronopotentiometric Analysis Of Cadmium(II) And Lead(II) Using Cysteine Modified Screen-Printed Electrode. <i>Cranfield University, UK</i>	17
- Electrochemical Method For The Rapid On-Site Screening Of Heavy Metals At Industrially Contaminated Sites. <i>Cranfield University, UK</i>	18
- Electrochemical Batch Injection Analysis Of Trace Metal Ions. <i>University of Coimbra, Portugal</i>	18
- pH/EC/TDS Measured By A Field Instrument On Waters And Soils From Aznalcollar Mining Area. <i>Geological Survey of Portugal</i>	19
- Development Of Chemical Sensors For Heavy Metal Detection In Environmental Matrices. <i>Cranfield University, UK</i>	19
- Urease-Based Biosensor For Heavy Metals Determination. <i>Cranfield University, UK</i>	20
- Lead Automatic Analyser (AQUAMET) <i>Universitat Autònoma de Barcelona, Spain</i>	20
- Luminescent Bacterial Sensors In Environmental Hazard Assessment. <i>University of Turku, Finland & National Institute of Chemical Physics and Biophysics, Estonia</i>	20
- In-The-Field Evaluation Of A Heavy Metal Analyser. <i>NMRC, Ireland & CIT, Ireland</i>	21
- Detection Of Heavy Metals Using Disposable Modified Electrochemical Sensors <i>University of Florence, Italy</i>	21
- Detection Of Toxic Compounds Using Disposable Electrochemical DNA Biosensor. <i>Univeristy of Florence, Italy</i>	22
- Bioluminescent Fiber Optic PMERRLUX, PARSRLUX Sensor. <i>Ben-Gurion University of the Negev and The Institute for Applied Biosciences, Israel</i>	22
- Pulse-Neutron Monitoring Tests On Aznacollar Site: Implications For Real-Time Pollution Detection And Integrated Environmental Monitoring. <i>Terramentor eeig, Finland</i>	22
- Screening Of Acute Biological Toxicity In Contaminated Sites With A Portable TOXALERT® 10 System. <i>Universidad de Alcalá, Madrid, Spain</i>	23
- PAHs, Chemical Analysis And Toxicity Screening By TOXALERT® 100. <i>IIQAB-CSIC, Barcelona, Spain</i>	23
Development requirements	24
DVD and video	25
Future prospects and recommendations	25

Press release	28
References	30
Annexes	31
Annex I. Announcement	32
Annex II. Preparation of samples for on site experiments	41
Introduction	42
Extraction and sample preparation for heavy metal analysis in Aznalcollar mining soil and sediments. <i>Gaona X, Pérez G, Colás E,</i> <i>Pacheco J and Valiente M</i>	43
Annex III. Results for each participant	47

1. Summary

The SENSPOL Technical Meeting on monitoring a contaminated metal mining site was organised in Sevilla, Spain 6-9 November 2002, by the EU projects on 'Improved Detection Systems for Toxic Heavy Metals in Contaminated Ground Waters and Soils' (DIMDESMOTOM) and 'Monitoring Environmental Pollutants in Water, Soil and Sediments' (SENSPOL), in collaboration with the Network for Industrially Contaminated Land in Europe (NICOLE) and Institute of Environmental Chemistry (IIQAB-CSIC), Barcelona, Spain. The goal of this unique site demonstration was to apply the latest sensing technologies at a site contaminated by metal mining activities.

The demonstration of modern sensing technologies took place at Aznalcollar, a former metal mining site near to Sevilla. Experts performed the sampling in September 2002 and detailed laboratory analyses were carried out at Autonomous University of Barcelona and at CSIC. However, these analytical results were not made available to participants until after the practical meeting. The meeting programme included an expert presentation and demonstration of a total process monitoring that included sampling, preparation and treatment of samples and a measuring step by the different participant instruments. In addition to extracts, untreated samples were also made available, together with extraction equipment. Most of the experimental work was performed in an old field laboratory building on the mining site. Some of the sensing devices were tested outside on the contaminated site.

Technology developers from eleven European countries were joined by representatives from industry, consultants and an environmental agency. Sixteen different instruments were brought to the site in a co-operative effort to demonstrate the applicability of new field measurement techniques. The devices demonstrated included commercial and non-commercial devices, and developments from EU and national programmes.

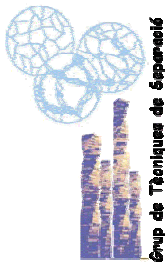
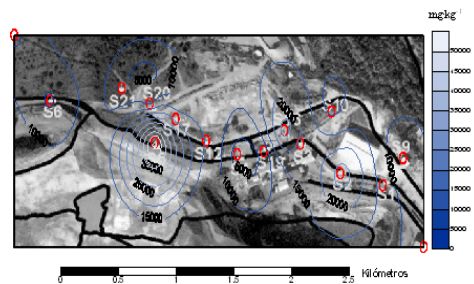
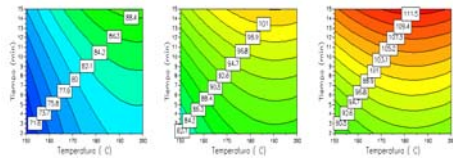
The on-site demonstration in Seville has resulted in a step forward in using new measuring techniques under field conditions. The instruments were used to successfully determine pollutants in soil, sediments and river waters at the contaminated metal mining site. Some provided indicative results within two days. The rapid field measurement techniques confirmed the effectiveness of the water treatment plant for mine wastes. They were also used to test for hydrocarbon contamination resulting from the use of fuel and flocculants during the mining activity. For the quantitative measurements of heavy metals, biosensors and chemical sensors have been optimised for particular target analytes, the most popular being cadmium and lead. A smaller number of techniques could also analyse copper, zinc, mercury and gold but with lower accuracy and higher detection limits than Cd and Pb. If the contaminants on a site are these metals then the existing tools are useful. The instruments have all shown their (potential) fieldability. One team processed 23 samples in two hours and if an extraction step could be developed to match that then these become very useful (and cost-effective) site screening tools.

A DVD/video of the event was made, it shows application of the latest sensing technologies and demonstrates their capabilities in addressing environmental problems in the field. The total monitoring process of collecting samples, preparation and the treatment necessary before a measurement can be made is addressed, and sensor devices are shown in operation.

The sensors and related analytical methodologies will bring savings in time and cost to current methods and extra information useful in solving environmental problems from heavy metal contamination. It can be concluded that these sensors have the potential for real applications in the assessment and management of contaminated land problems, not only as analytical techniques in their own right, but also as rapid and cost-effective screening tools. Further integration of new sensing tools into field screening however is dependent on increasing the availability to (end-)users and successful demonstration in projects.

Los estudios que se presentan en esta Tesis contribuyen a una mejora en la explotación de los resultados de la fraccionación de metales contaminantes como As, Cd, Cr, Ni, Pb o Zn en muestras de origen geológico contaminadas por la contribución antropogénica resultante de la explotación minera (Salsigne, Francia) o el tráfico rodado (Autopista C-58, España). La metodología de estudio se ha basado en el empleo de los procesos de extracción secuencial para la determinación de la disponibilidad de estos metales. Asimismo, se han empleado técnicas de análisis estadístico multivariable y herramientas geoestadísticas en combinación con la mencionada fraccionación para la obtención de posibles correlaciones entre los contaminantes y su movilidad, disponibilidad o persistencia.

Como paso previo a los estudios desarrollados dentro de la presente memoria, ha sido necesario el desarrollo, optimización y validación tanto de los Esquemas de Extracción Secuencial (SES) en sus formas convencional o acelerada (procesos monoetapa o ultrasonidos) como de las extracciones simples o los procedimientos de pseudodigestión por microondas analítico. Por otra parte se han estudiado los fenómenos de readsorción y redistribución de los metales contaminantes entre las diferentes fracciones evaluadas al aplicar los SES. Dichos fenómenos son considerados como uno de los principales inconvenientes de estos procedimientos de extracción secuencial dado que pueden conducir a una estimación errónea de los contenidos movilizados de los elementos contaminantes considerados.



CENTRE GRUP DE TÈCNiques DE SEPARACIÓ EN QUÍMICA
UNIVERSITAT AUTÒNOMA DE BARCELONA

EDIFICIO CN. FACULTAD DE CIENCIAS
BELLATERRA, 08193. BARCELONA.

Miembro de:
XIT XARXA DE CENTRES
DE SUPORT
A L'INNOVACIÓ
TÈCNICA
Red de Innovació